



Politecnico di Torino

MASTER'S DEGREE THESIS IN CIVIL ENGINEERING

Sustainability in construction: RSF fibers and their use in
structural concretes and mortars

Supervisors:

Alessandro Pasquale Fantilli (Polito)

Maurizio Taliano (Polito)

Carmine Galasso (UCL University)

Candidate:

Francesco De Falco (s317824)

Academic year 2024/2025

Abstract

The construction sector is therefore under increasing degree of pressure to adopt more sustainable methods of construction due to the enormous environmental impact brought forth by the traditional methods of concrete production: high CO₂ emissions; resource depletion; and excessive raw material extraction. Recycled steel fibers (RSFs), which provide potential solutions to these problems, are increasingly accepted as an eco-friendly alternative to enhance the performance of structural mortars and concrete. Being derived out of waste materials, RSFs are potential eco-friendly alternatives to conventional reinforcement methods, thus contributing to a Fiber-Reinforced Concrete (FRC) mix having less environmental footprint (the concept of using fibers from end-of-life tires illustrates how very important it is to recycle some items and the advantage they can impart in civil engineering). Also, on the other side, their application in civil engineering not only solves waste management problems but also enhances sustainability and performance attributes of structural materials. Further, with the development of new answers for environmental choices with cost benefits, this procedure sets the stage for a much more resilient and green construction industry.

Ringraziamenti

Voglio ringraziare i professori che mi hanno seguito durante il percorso di tesi, rendendo il lavoro più facile e leggero, con ottimi risultati.

Speciali ringraziamenti vanno ai miei amici, alla mia famiglia, i miei genitori, fratelli e nonni, zii, che mi hanno supportato durante tutto il percorso accademico, falli secchi....

Nulla di tutto questo sarebbe stato possibile senza la volontà di Dio. الحمد لله

Table of contents

Abstract	2
Chapter 1: Introduction	9
1.1. Sustainability in construction	9
1.2. Fiber reinforced concrete.....	10
1.3. Thesis objective.....	13
1.4. Thesis structure	14
1.5. Performance of FRC.....	14
1.5.1. Historical and modern references of FRC usage	18
1.6. Sustainable technologies of FRC and FRM	20
1.6.1. Sustainable supplementary cementitious materials	21
1.7. Durability of FRC.....	22
1.7.1. Durability studies of fiber reinforced concrete.....	22
1.7.2. Durability of hybrid fiber reinforced concrete (HFRC)	23
Chapter 2: Fibres	25
2.1. Types of Fibers and Their Uses	25
2.2. Steel fibers.....	27
2.2.1. Geometric and material parameters.....	27
2.3. Industrial and recycled technologies	30
2.3.1. Not all fibers have beneficial effects on mortars or concrete: insights and challenges	31
Chapter 3: Second life fibers from end life tires	35
3.1. Recycled steel fibers (RSF).....	35
3.2. Fibers from AGR Torino	36
3.2.1. Statistics.....	36
3.2. Fitting For Length, Diameter and Aspect Ratio	41
3.2.1. Qualitative analysis of distributions fitting	41
3.2.2. Goodness of fit tests	43
Chapter 4: Experimental analysis	46
4.1. Mix design.....	46
4.2. Samples preparation	49
4.3. Tests.....	53
Chapter 5: Results	56
5.1. Three point bending and compression test results.....	56
5.1.1. Calibration of the machine and measurements of the samples.....	57
5.1.2. Testing of the samples and failure study	58
5.1.3. Curves force-displacement	61
5.2. Comparison between industrial and recycled fibers.....	67
5.3. Tensile strenght.....	72

Chapter 6: Broken samples sections investigation	73
6.1. Fibers influence on broken sections	73
6.2. Relationship between beta, gamma and structural performance	77
Chapter 7: Conclusions.....	80
APPENDIX A.....	83
REFERENCES	94

List of Figures

Figure 1 differences in mechanical behavior between ordinary concrete (plain concrete NSC) and fiber-reinforced concrete (FRC) under uniaxial compression. [5]	14
Figure 2 splitting tensile test for concrete specimen	15
Figure 3: Load-displacement curve (P- δ) for fiber-reinforced composites characterized by (a) low fiber percentages and (b) high fiber percentages. [12].....	16
Figure 4: Load-displacement curve (P- δ): (a) degrading behavior and (b) hardening behavior. [5]	17
Figure 5 Tipu sultan’s palace.....	19
Figure 6 colosseum.....	19
Figure 7-Pueblo house.....	19
Figure 8 a Post-Damer Platz (by H. Falkner);b Oceanographic museum in Valencia (by P. Serna)`.....	20
Figure 9 fiber characteristics.	25
Figure 10 glass fibers	26
Figure 11 naturally occurring fibers	26
Figure 12 basalt fibers	26
Figure 13 steel fibers	30
Figure 14 compressive strenght based on polypropylene fiber dosage [13].....	33
Figure 15 Compressive strength comparison of PET-FRC, SFRC, and FGC mixes. [14]	34
Figure 16 dirty fibers on the left, cleaned final fibers on the right	35
Figure 17 steel fibres from AGR.....	36
Figure 18 probability density plot for length(a), and diameter of fibers(b)	38
Figure 19 scatter plot lenght vs diameter	39
Figure 20 fit distribution lenght of fibers	41
Figure 21 fit distribution for diameter of fibers	42
Figure 22 fit distribution for aspect ratio of fibers	43
Figure 23 mixer	50
Figure 24 industrial fibers	51
Figure 25 RSF from end-of-life tires.....	51
Figure 26 moulds oiled.....	51
Figure 27 filled molds with mortar	52
Figure 28 3-point bending test scheme	54
Figure 29 compression test scheme [30]	55
Figure 30 samples after 28 days of curing	56
Figure 31 Ref_1 sample after failure.....	59
Figure 32 Ref_1 sample before the test.....	59
Figure 33 R40_1 sample after failuree	60
Figure 34 R40_1 sample before testing.....	60
Figure 35 I40_1 sample at failure	60
Figure 36 I40_1 sample before testing	60
Figure 37 Ref_1 force-displacement curve (bending test).....	61
Figure 38 R40_1 force-displacement curve (bending test).....	62
Figure 39 I40_1 force-displacement curve (bending test)	63
Figure 40 Ref_1 sample before testing	64
Figure 41 Ref_1 after failure.....	64
Figure 42 R40_1 after failure	64

Figure 43 R40_1 sample before testing.....	64
Figure 44 Ref_1 force-displacement curve (compression test).....	65
Figure 45 R40_1 force-displacement curve (compression test).....	66
Figure 46 I40_1 force-displacement curve (compression test).....	66
Figure 47 histograms RI vs Rm flexural and compression	70
Figure 48 broken samples	73
Figure 49 n-Rmflexural.....	78
Figure 50 th- Rmflexural.....	78

List of Tables

Table 1 Differences between FRM AND FRC.....	13
Table 2 Differences between the types of fibre used in FRC AND FRM.....	26
Table 3 properties-units-standards for fibers.....	29
Table 4 Comparison of Industrial Steel Fibers and Second-Life Fibers	31
Table 5 statistic for L.....	37
Table 6 statistics for D.....	38
Table 7 fiber types and their volume	47
Table 8 mix design quantities.....	48
Table 9 plain and FRC response under loadings	55
Table 10 results from the three point bending test	67
Table 11 compression test results	69
Table 12 beta estimation.....	77

Chapter 1

Introduction

1.1. Sustainability in construction

Sustainability in construction has become an issue of major concern in the last years, the high pollution related to concrete production has put in danger the environment's health and safety, that is why construction regulations are going more and more towards a sustainable approach in the chosen materials[1]. To build environmentally friendly public constructions, authorities impose tailoring concrete mixtures with a minimum content of recycled materials. Concrete is the most environmentally demanding construction material in use worldwide[1]. A significant focus of this transition is the development and incorporation of eco-friendly materials that can replace traditional, resource-intensive components without compromising performance. Recycled Steel Fibers (RSFs) have emerged as a promising innovation in this context, offering a sustainable alternative for reinforcing mortars and concretes in structural applications. Fiber-Reinforced Concrete (FRC) and fiber reinforced mortar as well, can diminish the carbon footprint. As concrete infrastructure and building construction continue to expand, the production of concrete is increasing current environmental problems such as climate change, depletion of non-renewable resources, uncontrolled extraction of raw materials and emissions of polluting gases such as CO₂ within the atmosphere. Many companies are therefore moving towards a circular economy of concrete manufacturing where all the different stages of its production are being considered while trying to envision a net zero industry[1]. The Global Cement and Concrete Association (GCCA) has set the objective of a 40 % reduction in the carbon footprint by 2030 and to achieve net zero production by 2050[1]. The sustainability issue is so relevant that it is even addressed in the current concrete regulations. The European structural regulations (Eurocode 2 and Spanish Structural Codes) refer to the importance of that problem. The use of RSFs in construction exemplifies the synergy between performance and sustainability. By integrating RSFs into structural materials, the construction industry can progress toward greener solutions while maintaining safety and durability standards. This makes RSFs an essential component in the future of sustainable building practices.

1.2. Fiber reinforced concrete

Fiber Reinforced Concrete (FRC) is a type of concrete containing fibrous material which increases its structural integrity. It contains short discrete fibers that are uniformly distributed and randomly oriented. Fibers include steel fibers, glass fibers, synthetic fibers and natural fibers – each of which lend varying properties to the concrete.[2] In addition, the character of fiber-reinforced concrete changes with varying concretes, fiber materials, geometries, distribution, orientation, and densities. Fibers are used in concrete to control cracking due to plastic shrinkage and to drying shrinkage. RSFs are produced by recycling scrap steel, often sourced from end-of-life tires or other waste streams, thus addressing two critical environmental challenges: the accumulation of industrial waste and the extraction of virgin materials. These fibers not only reduce waste disposal issues but also contribute to circular economy principles by repurposing waste into valuable construction materials. Fiber-reinforced concrete is a composite material characterized by a cementitious matrix enhanced with short, discontinuous fibers made of steel, polymeric material, inorganic material (such as carbon or glass), or natural materials. Traditional or prestressed reinforcement can also be added on-site.

The weak matrix in concrete, when reinforced with steel fibers, uniformly distributed across its entire mass, gets strengthened enormously, thereby rendering the matrix to behave as a composite material with properties significantly different from conventional concrete. The incorporation of fibrous reinforcement in concrete is often evaluated from an economic perspective, as it reduces costs compared to traditional concrete by eliminating the time required for installing conventional reinforcement. Additionally, FRC offers practical advantages during casting, as the fibers are pre-mixed into the concrete. This makes it particularly suitable for producing secondary precast concrete elements, commonly used in civil and industrial construction as well as infrastructure projects. Because of the vast improvements achieved by the addition of fibers to concrete, there are several applications where Fiber Reinforced Concrete (FRC) can be intelligently and beneficially used. These fibers have already been used in many large projects involving the construction of industrial floors, pavements, highway-overlays, etc. [3]The principal fibers in common commercial use for civil engineering applications include steel, glass, carbon and aramid. These fibers are also used in the production of continuous fibers and are used as a replacement to reinforcing steel. High percentages of steel fibers are used extensively in pavements realization and in tunneling. This invention uses

Slurry Infiltrated Fiber Concrete (SIFCON). [3]Fibers in the form of mats are also being used in the development of high-performance structural composite. The usefulness of FRC in various civil engineering applications is indisputable. Fiber reinforced concrete has so far been successfully used in slabs on grade, shotcrete, architectural panels, precast products, offshore structures, structures in seismic regions, thin and thick repairs, crash barriers, footings, hydraulic structures and many other applications. [3]Concrete is most widely used construction material in the world due to its ability to get cast in any form and shape. It also replaces old construction materials such as brick and stone masonry. The strength and durability of concrete can be changed by making appropriate changes in its ingredients like cementitious material, aggregate and water and by adding some special ingredients. Hence, concrete is very well suitable for a wide range of applications. However, concrete has some deficiencies as listed below: 1) Low tensile strength, 2) Low post-cracking capacity, 3) Brittleness and low ductility, 4) Limited fatigue life, 5) Incapable of accommodating large deformations, and 6) Low impact strength. [3]The presence of micro cracks in the mortar-aggregate interface is responsible for the inherent weakness of plain concrete. The weakness can be removed by inclusion of fibers in the mixture. Different types of fibers, such as those used in traditional composite materials, can be introduced into the concrete mixture to increase its toughness, or ability to resist crack growth. The fibers help to transfer loads at the internal micro cracks. Such concrete is called fiber reinforced concrete (FRC) (Shende et al. 2012). Steel fibers are the most used for concrete reinforcement. Flooring and tunnelling are the main applications of fiber reinforced concrete (FRC). The elastic properties and compressive strength of the cementitious matrix are not significantly affected by the presence of fibers (except when used in high percentages), unlike the mechanical properties, which are significantly influenced. The addition of fibers improves the mechanical properties of concrete, primarily due to the development of post-cracking resistance, which is typically absent in a matrix without fibers and is the basis for structural design of FRC elements. [4]

As soon as micro-cracks form in the concrete, the fibers are activated, counteracting the progressive opening of the cracks and generating significant residual tensile strength in combination with substantial deformation effort. This results in an increase in ductility (advantageous especially for hyperstatic structures) and toughness (the energy required to break the composite under tension). What mentioned above can be clearly seen in the figure 1 reported below, clearly a matrix with such a big amount of fibers leads to an heavy improvement on

deformation characteristics, almost looking like steel , providing a technology of important endurance and specifically for heavy loads applications.

Conversely, fiber-reinforced mortar is a composite material made of fibers (such as steel, synthetic, or natural fibers), fine aggregates (usually sand), cement (as a binder), and water.

Applications where the lack of coarse materials (such as gravel) is required employ FRM. By adding fibers, the naturally brittle mortar's tensile qualities are improved, and breaking brought on by drying shrinkage or outside forces is lessened.

FRM's characteristics

A higher tensile strength, fibers bridge cracks as they appear, lowering the chance of brittle failure. [4]

Durability is improved by increasing resistance to environmental conditions such freeze-thaw cycles, abrasion, and chemical attack.

Fibers aid in preventing microcracks from spreading into more significant structural defects. FRM is particularly suited to situations where thin sections, repair, or finishing layers are required.

Common applications include:

1. Restoration of deteriorated concrete structures.
2. Filling and patching of cracks or spalled areas.

Seismic Retrofitting:

Strengthening walls, columns, and other load-bearing elements in earthquake-prone areas.

Thin Overlays and Coatings:

Applied as protective or decorative finishes.

Used for pavements, facades, or marine structures.

Shotcrete for Lightweight Construction:

For slope stabilization, tunnels, or domes.

Table 1 Differences between FRM AND FRC

Aspect	FRM	FRC
Aggregate	Fine aggregates only (sand)	Fine and coarse aggregates (sand + gravel)
Thickness	Typically used for thin applications	Suited for thicker structural elements
Applications	Repairs, overlays, retrofits	Load-bearing structures, industrial floors
Fiber Role	Mainly controls shrinkage cracks and microcracks	Enhances toughness, ductility, and impact resistance
Strength Impact	Minor improvement in load-bearing capacity	Significant enhancement in structural capacity

Crack management involves using fibers to bridge cracks, lowering their width and enhancing service life. Improved Toughness and Ductility: FRC and FRM exhibit a progressive failure mode. Making them safer and more predictable during stress.

Reduced maintenance costs, reduced cracks lead to less water penetration and corrosion, increasing structure lifespan.

1.3. Thesis objective

Our study focuses on how to implement new technologies in the construction field that might help reduce the environmental impact of concrete, trying to evaluate steel fibers performance in a mortar/concrete mixture. Furthermore, with the recycled fibers from end life tires, received from an industry, the aim is to check the quality of the product, prove if the recycled fibers behavior is good enough to replace the industrial fibers, making a performance comparison, and potentially put in bigger future applications, as well as see if further investments in this type of technology would be beneficial and can be applied in the construction industry.

In order to do so, it has been of primary importance checking all the regulations involved in such research, aiming to get final values that comply with the law requirements and standards, checking if the final product satisfies the expected results.

1.4. Thesis structure

In chapter one, we illustrated the definition of FRC and the related benefits, as well as its performance and regulations. In addition the objective of this thesis were introduced. In Chapter two there has been described fibers and various typologies used for structural purposes. In Chapter three there were described the RSF from end life tires, with a s relative statistical study. Then in Chapter four, these fibres were put into a mix design for mortar samples, preparing a proper mixture that will be tested. In Chapter five, the produced samples were tested and their results analyzed , to see what went fine and what went wrong. In Chapter six, the broken samples were taken for further investigations, and in the last Chapter, number seven, there are the conclusions.

1.5. Performance of FRC

To evaluate the performance of FRC , tests are performed and curves are plotted.

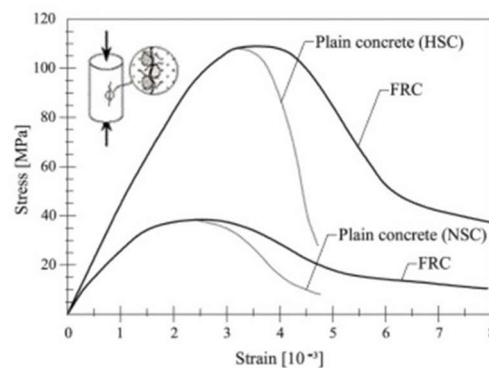


Figure 1 differences in mechanical behavior between ordinary concrete (plain concrete NSC) and fiber-reinforced concrete (FRC) under uniaxial compression. [5]

The mechanical behavior of fiber-reinforced concrete (FRC) and plain concrete under uniaxial compression is explained by this plot. Both high-strength concrete (HSC) and normal-strength concrete (NSC) are included. [5]

When plain concrete (NSC) reaches its maximum stress, it shows a brittle failure and a decreased peak stress and strain.

By adding fibers, the material becomes much more ductile and can withstand stress over a wider range of strains once the peak stress is attained. This indicates that the FRC absorbs energy more efficiently and resists fracture.

Compared to NSC, plain concrete (HSC) has a larger peak stress but is still brittle and loses stress quickly after reaching its maximum. FRC (HSC): The addition of fibers in high-strength

concrete improves both post-peak ductility and energy absorption capacity, though to a lesser extent than in NSC.

The graph demonstrates how fibers improve the performance of concrete; in fact it determines an increased toughness and resistance to cracking. Better energy dissipation during loading. Enhanced ability to maintain structural integrity under stress. Illustration of Compression: The inset diagram shows a cylindrical specimen under uniaxial compression, visually representing the test setup used to obtain the stress-strain curves.

To determine how concrete behaves under tensile loading (forces pulling it apart). Because concrete is naturally weak under tensile stress, it can be strengthened with reinforcing, but tensile testing is essential.

The load-displacement curve for plain concrete displays a significant peak in the plot:

Elastic deformation is represented by the first linear segment, in which the material undergoes reversible deformation.

The peak load is the maximum tensile load that plain concrete can sustain before cracking.

After the peak, the load drops sharply, indicating that cracks propagate rapidly through the material, leading to a sudden and catastrophic failure. This is typical of plain concrete under tension.

Another important way to verify the performance of FRC is the splitting tensile test, here reported below a figure of a sample under loading.



Figure 2 splitting tensile test for concrete specimen

The splitting tensile test, also known as the Brazilian tensile strength test, is a standardized technique for assessing concrete's tensile strength. Since concrete is weak under stress and direct tensile testing can be challenging, this test provides an indirect way to assess the tensile strength. [6] A compressive force is applied along a cylindrical concrete specimen's diameter during the test. [6] Tensile stresses are produced when the load is compressive, and the stresses are induced perpendicular to the load direction. In order to replicate the tensile failure, these stresses lead the specimen to split along its diameter. [6]

There is a noticeable decrease in compressive brittleness, especially with high-strength concretes. An FRC's cementitious matrix is made out of mortar or concrete. The granulometry of the matrix must be carefully planned, with special emphasis to the fine fraction of the aggregate, to guarantee good workability of the mixture and successful bonding with the fibers. The physical and chemical properties of the cementitious matrix and its components must comply with the reference standards applicable to fiber-free concrete. Unlike traditional reinforcement with steel bars, the added short fibers usually do not increase the compressive strength of the concrete. However, thanks to their homogeneous diffusion, they are more effective in improving the post cracking behavior of the concrete element. Their purpose is therefore to increase the ductility and capacity to absorb energy, through the control of crack propagation. The main components of the matrix in FRC do not vary compared to those of traditional cementitious materials, which are typically: Portland cement, water, aggregates of

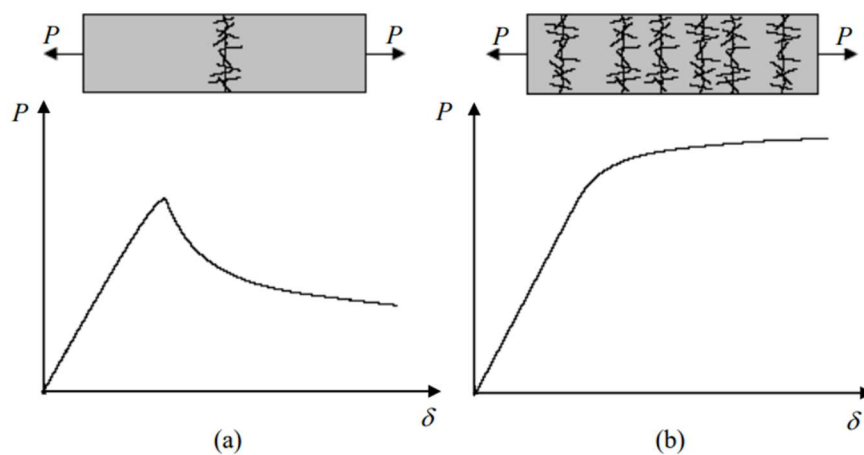


Figure 3: Load-displacement curve ($P-\delta$) for fiber-reinforced composites characterized by (a) low fiber percentages and (b) high fiber percentages. [12]

various sizes, and additives. The choice of quality of the components and their proportions in the mixture depend on the main requirements of strength grade, workability at the fresh state,

porosity, and durability. Essentially, the matrix generally consists of Portland cement-based concrete when low amounts of fibers are added.

As was seen above, fiber-reinforced concrete (FRC) exhibits distinct behavior under tensile loading compared to ordinary concrete.

It can be mentioned two behaviors:

The degrading behavior reflects poor energy absorption and is characteristic of materials with insufficient fiber reinforcement or inadequate fiber properties.

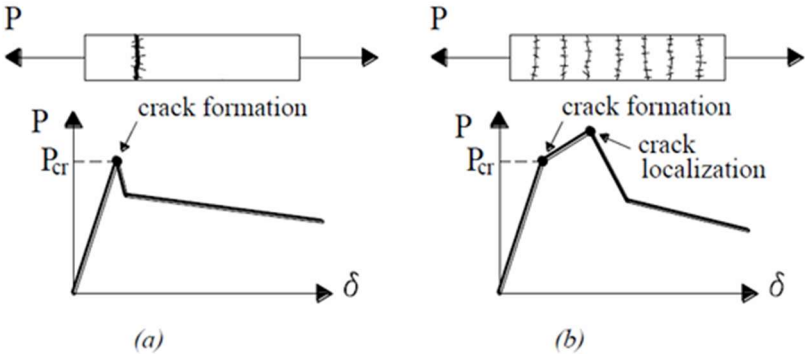


Figure 4: Load-displacement curve ($P-\delta$): (a) degrading behavior and (b) hardening behavior. [5]

Hardening Behavior, on the other hand, demonstrates enhanced toughness and durability, making it ideal for high-performance applications in structural engineering, such as seismic-resistant structures.

Materials with weak fiber-matrix bonding or low fiber content typically exhibit this behavior(a). The fibers lose their ability to support weight when the matrix breaks because they are unable to adequately bridge the fracture.

Conversely, a different curve similarly starts in an elastic area and ends at P_{cr} at the first fracture. However, because the fibers bridge the fissures, the load capacity later rises rather than falls. Crack localization happens as the stress increases, ultimately resulting in a plateau. These curves highlight the importance of tailoring the fiber content, type, and matrix properties to achieve the desired structural performance. The transition from degrading to hardening behavior is a key objective in designing advanced FRC systems for various civil engineering applications. The structural use of FRC is governed by various regulations published over recent years. In Italy, one of the first documents on the subject is the CNR-DT 204/2006, “Instructions for the design, execution, and control of fiber-reinforced concrete structures”, which primarily

references the recommendations outlined in RILEM (2003), “Test and design methods for steel fiber-reinforced concrete”. However, subsequent studies and the publication of the Model Code 2010 have led to the development of more updated texts, namely the Guidelines issued by Consiglio Superiore dei Lavori Pubblici (hereinafter CSLPP) and the new version of Eurocode 2, Part 1-1 (2022). The current Technical Standards for Construction 2018 (hereinafter referred to as NTC18) state that:

"Both for the qualification of fiber-reinforced concrete and for the design of FRC structures, exclusive reference must be made to specific provisions of the High Council of Public Works, issued through dedicated Guidelines," namely:

"Guidelines for the design, implementation, control, and testing of structural elements in fiber-reinforced concrete with steel and polymeric fibers" (hereinafter referred to as LG2022)] and

"Guidelines for the identification, qualification, technical assessment certification, and acceptance control of FRCs" (hereinafter referred to as LG2019). The same guidelines apply to Fiber Reinforced Mortars as well.

1.5.1. Historical and modern references of FRC usage

It is used on account of the advantage of increased static and dynamic tensile strength and better fatigue strength. FRC is

used for [5]:

- Runway, Aircraft parking and Pavements
- Industrial flooring
- Tunnel and canal lining
- Slope stabilization
- Thin shells
- Curtain Walls
- Pipes
- Manholes
- Dams and Hydraulic structures
- Roof tiles
- Composite decks
- Impact resisting structures [7]

There are many reasons why such uses are effective with FRC technologies, in fact due to its ability to withstand heavy loads, particularly regarding rigid pavements used for taxiways or railways, gives high reliability in terms of thermal stresses, as well as water pressure resistance

like in dams or canals.[7] Because of its great tensile strength and crack resistance, FRC enables the production of thin, lightweight yet strong shells, allowing for novel architectural designs. Moreover it is a flexible material that gives the opportunity to engineers to have a wider range of uses without facing too many difficulties. The concept of employing fibers for reinforcement trace back to decades of years ago. In ancient times, horsehair was used in mortar and straw in mud bricks. In the 1900s, asbestos fibers were utilized in concrete. However, asbestos use was discouraged due to health concerns. In 1963, Romualdi and Botson released their seminal study on FRC. After that, other materials such as steel, glass, and synthetic fibers replaced asbestos in concrete.[7] This technology continues to be researched. FRC is regarded one of the most significant advances in construction engineering. Some instances or renowned constructions built using the FRC system built around 1540 using straw reinforcement. [7]

Use of horsehair in plaster has many historical references [7]



Figure 6 colosseum



Figure 5 Tipu sultan's palace



Figure 7-Pueblo house

Here below are reported some pictures of various applications of FRC in modern structures:



Figure 8 a Post-Damer Platz (by H. Falkner);b Oceanographic museum in Valencia (by P. Serna)`)

The primary difficulty remains the creation of trustworthy design equations that account for the function of short, discrete, and discontinuous fibers in diffuse reinforcement[8]. These fibers increase the performance of cementitious composites by increasing residual strength at tiny crack widths, especially in serviceability limit states. Furthermore, they help to increase the final load-bearing capacity of buildings during bigger crack openings by partially substituting standard steel reinforcement. In some circumstances, especially with a high fiber content, fibers can completely replace traditional steel reinforcement, resulting in hardened bending behavior.

This approach is especially advantageous for thin structural elements, where conventional reinforcement is difficult to implement due to the required minimum cover for durability. [8]

1.6. Sustainable technologies of FRC and FRM

One way to reduce the environmental impact of concrete production is to use green fuels derived from renewable sources[1], treat industrial waste through organic pollutant degradation, and use advanced gas treatments such as biogas upgrading[1], hydrogen storage, and NOx reduction[1]. Furthermore, replacing conventional raw materials with more ecologically friendly alternatives, particularly binders, is an important step toward lowering concrete's environmental footprint, as binders contribute significantly to the overall impact. Current study is looking into waste recycling and reuse across multiple industries to replace cement and aggregate quantities in concrete. Industries can improve their sustainability by reusing industrial byproducts as raw materials, while the construction sector can manufacture eco-friendly materials from construction and demolition waste. [1]

In the majority of studies, the Global Warming Potential (GWP), also referred to as Climate Change or the Greenhouse Effect, emerged as the most significant environmental impact. Cement consistently accounted for the largest share of GWP in FRC production, with concrete without fibers averaging a GWP of 320 kgCO_{2e}/m³ [1]. Conventional fibers also contributed notably to GWP, particularly steel fibers, which had a GWP of 2.6 kgCO_{2e}/kg [1], approximately three times higher than that of cement[1]. However, the overall GWP of FRC was typically not significantly higher, as the proportion of fibers in the mix was much smaller compared to that of cement, which was the primary source of environmental impact. Additionally, the required admixtures played a role in the total GWP. Most FRC mixtures, however, tended to achieve lower GWP values compared to reference mixtures, as efforts were made to enhance sustainability by selecting specific fiber types or optimizing the fiber production process.

1.6.1. Sustainable supplementary cementitious materials

Fly ash and slag, as sustainable supplementary cementitious materials, further support these efforts by replacing a portion of traditional cement in concrete. These industrial by-products not only reduce the reliance on raw materials but also enhance durability and mechanical performance. Fly ash improves workability and long-term strength, while slag contributes to higher resistance to chemical attacks and thermal stability.[9] Both materials significantly lower carbon dioxide emissions associated with cement production and integrate seamlessly into fiber-reinforced and waste-recycled concrete systems, creating a powerful synergy for greener construction solutions. This integration of fly ash, slag, recycled materials, and fibers represents a multifaceted strategy to develop more sustainable, high-performance concrete.

What happens if what mentioned above is combined, a very low emission mix design might come out from it, a study investigates the use of steel fibers (SF) in alkali-activated fly ash/slag (AAFS) mortars to enhance their mechanical properties, electrical conductivity, and self-sensing capabilities.[9] These materials aim to replace traditional Portland cement mortars, offering both environmental and functional benefits.

Since the binder is the first responsible for pollution, if it is completely or partially replaced with an industrial by-products (like slag and fly ash), the emissions can be significantly be reduced, even by 80% ,compared to traditional Portland cement.[9]

Steel fibers (\$5 per kg at) could provide an extremely cost-effective alternative to very expensive materials such as graphene, and at the same time, these inexpensive materials are put to very good use in enabling conductivity and enhancing mechanical performance.

The inclusion of 1 vol% steel fibers reduced the resistivity by an order of magnitude, which is certainly sufficient to allow their application in the making of smart multifunctional materials.[9]

In conclusion, SF-AAFS mortars combine sustainability with advanced sensing and structural performance. The ability to monitor stress, detect cracks, and maintain mechanical integrity positions them as a promising material for self-sensing, smart concrete structures in modern construction.

1.7. Durability of FRC

1.7.1 Durability studies of fiber reinforced concrete

Fiber reinforced concrete (FRC) reflects high durability; the reason is that various fibers have been incorporated into its matrix to improve mechanical properties against environmental degradation and to enhance structural performance. Steel fibers and non-steel fibers, such as cellulose fibers, polyvinyl alcohol fibers, and polyolefin fibers, are significant for improving durability in concrete.

Steel fibers work to improve post-peak behavior, fracture toughness, and crack-bridging ability of concrete, as well as reducing its permeability as a result of the inhibition of crack and microcracking growth. Besides, they provide SFRC the bonding ability for crack bridging and sealant for fissures against the continuous freeze-thaw application. Therefore, it offers an extreme high resistance against such weathering conditions.

Electrical Resistivity and Corrosion: The electrical resistance of concrete is decreased by the addition of steel fibers, which also might cause a higher sulphate and corrosion attack. However, by limiting cracking and microcracking, these fibers delay the ingress of chloride ions and enhance the short-term durability of concrete.

Afroughsabet & Ozbakkaloglu [10] stated that while steel fibers decrease the electrical resistivity of concrete significantly, they also enhance crack resistance.

Nahhab & Ketabb [10], [11] found that additional micro-steel fibers in the mix resulted in lesser drying shrinkage but increased pore water permeability to some extent.

Non-steel fiber reinforcement:

Other fibers used for enhancing durability in FRC include cellulose fibers (CTF), polyvinyl alcohol fibers (PF), and polyolefin fibers (VS). These fibers also grant dissimilar advantages, particularly regarding resistance against penetration of chloride ions. Lin and Cheng found that polyolefin fibers extend the time before the chloride ions reach the surfaces of the rebars, thus reducing initial corrosion rates.[10] Such characteristics represent a key support against degradation processes which concrete might suffer, when it comes to design in aggressive environments these types of fibers might be potentially good choices for a better performance and less risk of catastrophes.

1.7.2. Durability of hybrid fiber reinforced concrete (HFRC)

It incorporates hybrid fibers, steel fibers, and other types of fibers. These two fibers complement each other, optimally harnessing the strengths of each fiber toward the improved durability of concrete.

Advantages of Hybrid Fibers:

- Delay in the initiation of corrosion due to crack resistance improvement.
- Improved resistance to penetration of chloride ions, drying shrinkage, and impacts.
- Improvement in abrasion resistance through synergistic combination of macro and microfibers.

The researchers Afroughsabet and Ozbakkaloglu stated that 0.3% addition of polypropylene fibers with 0.7% steel fibers resulted in the least water absorption capacity in differing FRCs [10]

That a hybrid mix of macro synthetic fibers and polypropylene fibers resulted in improved chloride-ion penetration resistance compared to micro synthetic fibers alone, according to the authors Kim et al. [10].

Fiber addition, whether steel or otherwise, reduces drying shrinkage and extends the time in which cracking tends to begin. For instance, Yousefieh et al.[11] defined steel, polypropylene, and polyolefin fibers as putting off the earliest initial cracking timing.

Water permeability and chloride-ion penetration: Fiber incorporation reduces permeability since the structure of the pores is refined. An excess of fiber, however, damages the matrix, affecting the resistance of the matrix to chloride-ion erosion, according to Kim et al. [10]

These improve freeze-thaw durability through fiber crack control, which limits water ingress, thus protecting the material from damage due to repeated expansions and contractions. Microscopic studies show the mechanism of interaction between the fibers and the cement matrix: fibers bridge cracks, decrease pore connectivity, and limit access of harmful elements into concrete. Such micro understanding is important to optimize the fiber dosage as well as a proper trade-off among durability performance parameters.

In conclusion, the combination between steel fibers with non-steel fibers such as cellulose, polyvinyl alcohol, and polyolefin fibers would be one of the most promising routes toward increasing the durability of FRC. A hybrid fiber system can give engineers the advantage of an all-around mechanical performance, crack resistance, and environmental durability. Future research on the amounts of fiber and combinations would help with designing more durable and more sustainable concrete structures of different applications.

Chapter 2

Fibres

2.1. Types of Fibers and Their Uses

Modern concrete technology is made possible using fibers, which ensures that concrete is transformed, regarding how it behaves under stress and in hostile environments. Fiber-reinforced concrete (FRC) consists of adding discrete fibers into the concrete mix for the development of mechanical properties like tensile strength, ductility, and crack resistance. In contrast to ordinary plain concrete, which is brittle and has a higher tendency to crack under tension, FRC has modified some properties by using various unique fibers for justifying durability and performance in many applications. There are many types of fibers available for FRC ranging from synthetic (such as polypropylene, carbon fibers, etc.), natural (including jute and coir), and metallic or mineral-based fibers (including steel and basalt). However, each type of fiber has its advantages, which helps address specific needs for structural and non-structural applications, including concerns with shrinkage cracking, impact resistance or even sustainability. [7]The advantage of fibres is that it can be used by engineers to design concrete solutions that are made stronger, tougher and greener. There is a very large variety of fibers, ranging from different materials and geometry, mechanical characteristics and performance. Natural, synthetic, and sophisticated fibers are utilized in concrete, each of them have its own set of advantages and disadvantages.[7]

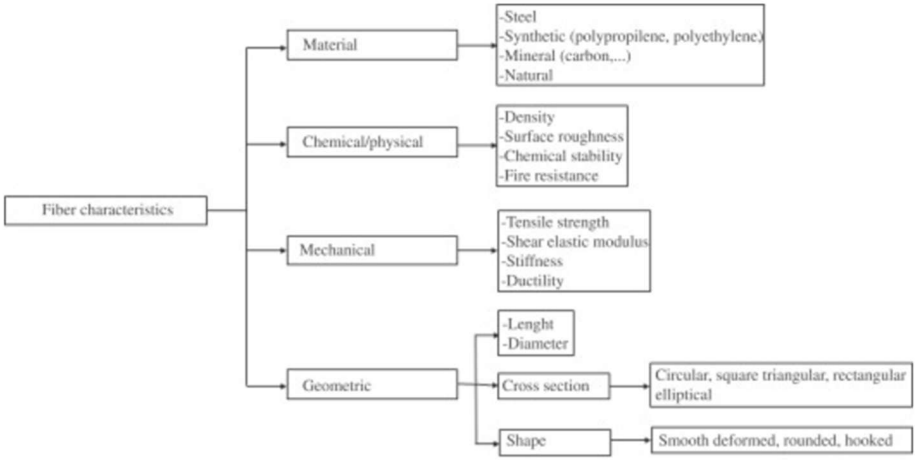


Figure 9 fiber characteristics.

Waste plastic fibers (e.g., PET) and polypropylene fibers are environmentally friendly and improve crack resistance, although they have low structural performance. Carbon and basalt fibers have excellent tensile strength and endurance, making them useful in high-performance and fire-resistant concrete.[7] However, they can be expensive and have unknown long-term performance. Glass fibers increase durability and are corrosion resistant, whereas natural fibers such as jute and coir are environmentally beneficial but degrade over time. Hybrid fibers combine components to improve fracture control and strength but are more expensive and difficult to employ.[7]



Figure 11 naturally occurring fibers



Figure 10 glass fibers



Figure 12 basalt fibers

Table 2 Differences between the types of fibre used in FRC AND FRM

Fiber Type	Tensile Strength	Durability	Cost	Applications
Waste Plastic Fibers	Low to moderate	Moderate	Low	Eco-friendly and non-structural
Polypropylene Fibers	Moderate	High	Low	Shrinkage control, fire resistance
Carbon Fibers	Very high	Very high	High	High-performance concrete
Glass Fibers	High	Moderate	Moderate	Architectural applications
Natural Fibers	Low to moderate	Low	Low	Rural construction
Basalt Fibers	High	High	Moderate	Marine, fire-resistant concrete
Hybrid Fibers	Very high	High	High	Specialized applications

2.2. Steel fibers

Steel fibers are the most used fibers. Steel fiber reinforced concrete is basically cheaper and easier to use a form of rebar reinforced concrete. Rebar reinforced concrete uses steel bars that are laid within the liquid cement, which requires a great deal of prep work but make for a much stronger concrete. Steel fiber reinforced concrete uses thin steel wires mixed in with the cement. Generally, round fibers are used.

2.2.1. Geometric and material parameters

Steel fibers are characterized not only by their material composition but also by their geometric parameters, such as length, equivalent diameter, aspect ratio, and shape. The production of steel fibers must comply with qualified procedures and use certified materials. Specifically, fibers must bear the **CE marking**, in accordance with the harmonized European standard **EN 14889-1**, and their packaging must indicate the production batch.

The following parameters are defined by the harmonized standard:

Fiber Length

The fiber length, denoted as l_f , is defined as the distance between the ends of the fiber. The axis length of the fiber is identified as the developed length l_d . The measurement of fiber length must adhere to specific reference standards. Steel fibers generally have a length l_f ranging between 6 mm and 70 mm. [5]

Equivalent Diameter

The equivalent diameter, denoted as d_f , is defined as the diameter of a circle with an area equal to the average cross-sectional area of the fiber. Steel fibers typically have an equivalent diameter ranging between 0.15 mm and 1.20 mm. [5]

For fibers with circular cross-sections and a diameter greater than 0.3 mm, the equivalent diameter must be measured using a micrometer in two approximately orthogonal directions, with a precision specified by reference standards. [5] The equivalent diameter is then obtained as the average of these two measurements.

For fibers with a diameter smaller than 0.3 mm, the diameter must be measured using optical instruments, with precision specified by reference standards.[5]

For elliptical cross-sections, the equivalent diameter is evaluated based on the measurements of the two axes, performed with a micrometer according to established precision standards. The equivalent diameter is calculated as the average of the two axes' lengths.[5]

For rectangular cross-sections, the width b_f and thickness h_f of the fiber must be measured as specified by the applicable reference standards.[5]

$$d_f = \sqrt{\frac{4 * b_f * h_f}{\pi}} \quad [5] \quad (2.1)$$

For fibers with irregular cross-sections, the equivalent diameter can also be calculated based on specific relationships that take into account parameters like mass (m), developed length (l_d), and density (ρ_f).

$$d_f = \sqrt{\frac{4 * m}{\pi * l_d * \rho_f}} \quad [5] \quad (2.2)$$

Aspect Ratio

The aspect ratio is defined as the ratio of the fiber length l_f to its equivalent diameter d_f . [5]

Shape

Fibers may have various shapes, including straight or deformed forms, such as hooked, crimped, or waved designs. [5]

Elastic Modulus

The elastic modulus of the fiber must be evaluated in accordance with specific reference standards. [5]

Tensile Strength

The tensile strength of the fiber is the stress corresponding to the maximum tensile force the fiber can withstand. This property must be evaluated following specific reference standards, as the ratio between the maximum force and the equivalent cross-sectional area, defined as the area of a circle with diameter d_f . The table provided in the standard includes indicative tensile strength values for steel fibers, where R_m and $R_{p0.2}$ represent, respectively: [12]

- Ultimate tensile strength (UTS): Corresponding to the maximum load capacity. [12]
- Yield strength at 0.2% offset: Representing the stress at which the fiber exhibits a 0.2% non-proportional elongation. [12]

Table 3 properties-units-standards for fibers

Property	Unit of Measurement	Designation / Reference Standard
Shape	-	Hooked/twin-core
Material Density	[g/cm ³]	ρ_f / EN 14889
Length	[mm]	l_f / EN 14889
Diameter	[mm]	d_f / EN 14889
Crystal Melting Temperature	[°C]	T_m / 11357-3-2013
Tensile Strength	[MPa]	f_t / EN 14889
Elastic Modulus	[GPa]	E_f / EN 14889
Elongation at Break	[%]	A_{ft} / EN 14889

Two primary categories of steel fibers are widely utilized in FRC and FRM: industrial fibers and second-life fibers.



Figure 13 steel fibers

2.3. Industrial and recycled technologies

Recent advancements in Fibre-Reinforced Concrete (FRC) include the development of new fibre-matrix systems, such as:

1. High-Fiber-Volume Micro-Fiber System

This is a system that can provide a green substitute in place of asbestos fibers. Have improvement qualities of toughness and impact resistance; thus, it is most suitable for thin precast products like roofing sheets and cladding panels.[5] Cement composites incorporating this system are particularly suitable for repair and rehabilitation projects because of their extraordinary durability and strength.

2. Compact Reinforced Composites CRC

CRC presents a very dense, strong cement matrix, yet it is extremely expensive. With flexural strength reaching up to 260 MPa and compressive strength around 200 MPa, it has remarkable mechanical properties.[7]

Strength corresponding to structural steel allows direct molding and manufacturing on sites of construction, where design flexibility and application vary.

3. Polymer Concrete

Traditional polymer concrete suffers from porosity due to air and water voids.[7] A newly developed technique of impregnating with a monomer followed by polymerization dramatically

reduces porosity and improves strength and durability. These developments indicate the ever-increasing scope within fiber-reinforced systems to improve performance for concrete in various applications.

Table 4 Comparison of Industrial Steel Fibers and Second-Life Fibers

Aspect	Industrial Steel Fibers	Second-Life Fibers
Material	High-strength steel	Recycled plastic, textile, or tire materials
Strength	High tensile and impact resistance	Lower tensile strength, better flexibility
Durability	Resistant to heavy loads and harsh conditions	More suitable for light-duty or decorative applications
Eco-friendliness	Less eco-friendly, requires energy-intensive production	Highly sustainable, repurposes waste
Applications	Structural and heavy-duty applications	Non-structural or light-duty applications
Cost	Higher due to material and manufacturing costs	Lower and more economical

The fibers can partially or totally replace ordinary and reinforcing bars consequently improve the behavior at the Ultimate Limit State but also increase the durability and reduce the depth of cracks, i.e. improve state behavior serviceability limit.

2.3.1. Not all fibers have beneficial effects on mortars or concrete: insights and challenges

Once in advance of repeating the test run, it was determined that not all fibers have an identical positive influence when promoting some mechanical and durability characteristics; for example, the offered amount of fibers how interacts with the matrix. The other reason determining the behavior of the fiber-reinforced mortar is depending upon the selection of the fiber, its characteristics and the amount of mortar, and how well it interacts with the cement matrix. The focus of the present study is the assessment of the use of polypropylene fibers as an additive in cement mortars with respect to compressive strength. Fibers were added to mortar

mixes in different combinations of cement and sand (1:2, 1:3, and 1:4) and different dosages (0.1%, 0.5%, 0.75%, and 1%) based on the weight of cement. [13] The applicability of these mortar mixes for structural repairs and retrofitting was tested, especially with respect to their capacity to improve crack resistance, tensile strength, and durability.

Material Constitution:

- Cement-The cement used was of 53-grade OP cement fabricated with properties by IS standards.[13]
- Fine Aggregates: M-sand was tested for specific gravity, water absorption, and bulk density.
- Fibers: Polypropylene fibers (12 mm long, a triangle with a high aspect ratio).
- Water: Potable water was used as per IS standards. [13]

Testing Procedure:

- The mortars were cast with constant water content and tested after 28 days of curing.
- The compression test was conducted according to IS standards on cube specimens.

Results:

High fiber contents caused reductions in compressive strength across all ratios due to a balling effect at high fiber dosages. The 1:3 mix ratio performed better than the other two proportions in achieving a right balance between workability and strength. [13]

Applications:

- Fiber-reinforced mortars are effective for retrofitting and repairing weak structural elements. [13]
- Suitable for non-structural and structural purposes, such as crack resistance and durability enhancement.[13]

Even though in all case with the increase of fibers percentage there is a decrease in mechanical performance, among the studied case the 1:3 mortar is the case where the reduction is smaller, compared to 1:2 mortar which has more cement content and 1:4 which has less cement content.

Obviously, higher the cement content, higher is the compressive strength but the middle case find a balance between the samples. Nevertheless, in all cases of this study, polypropylene fibers have a negative impact on structural performance, such results prove that it is no guaranteed to

have a beneficial effect on a mix design of adding fibers, a specific and detailed study of the mix design is required for these purposes.

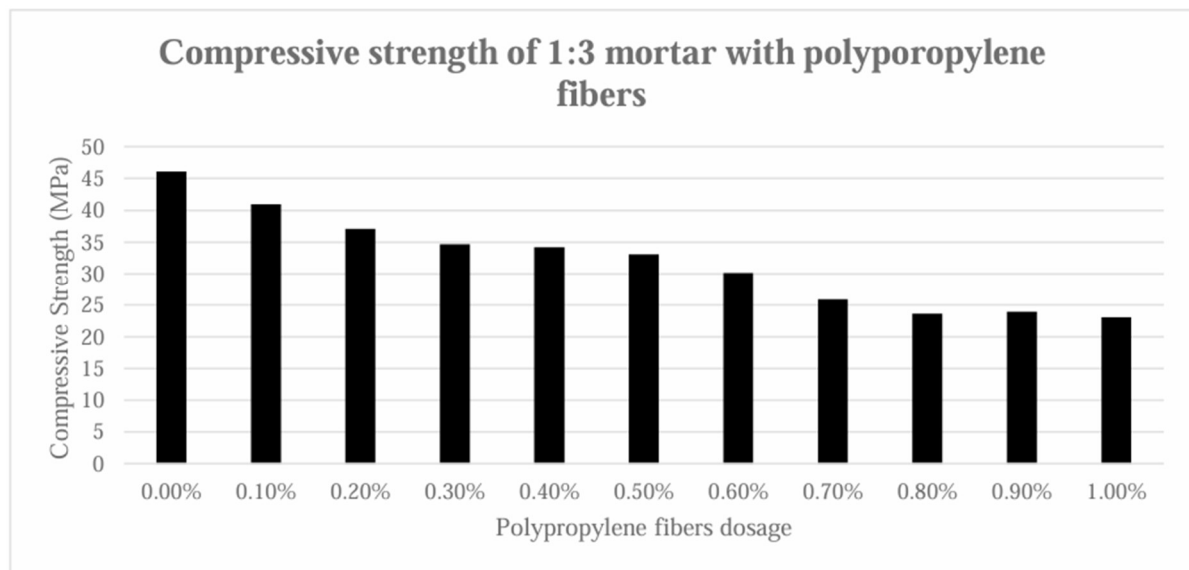


Figure 14 compressive strenght based on polypropylene fiber dosage [13]

Another study has shown that PET fibers have both negative and positive effects in structural performance:

PET fibers enhance flexural strength positively, in contrast to Plain Cement Concrete (PCC). The tensile strength is improved since cracks under bending stress are arrested by the fibers, thereby contributing to the toughness and ductility of the concrete.

Disadvantages of PET Fibers:

The detrimental effect of PET fibers on compressive strength is a very important drawback, and this property is exceedingly important for structures like columns, foundations, and load-bearing walls. The study shows that the compressive strength of PET-FRC (Fiber Reinforced Concrete) was reduced by 42.4% compared to that of PCC, thus not acceptable in high-load applications.[14] PET fibers also perform poorly under tension, showing 17.1% lower split tensile strength than PCC.[14] And the environmental attack coming from high temperatures or alkaline areas makes them very susceptible to degradation , which might reduce concrete's life span.

Without doubt, SFRC significantly outperform other mixes demonstrating to be the best option in this type of technology, nevertheless using other types of fibers might be a more sustainable choice, especially when fibers come from waste products or recycling processes.

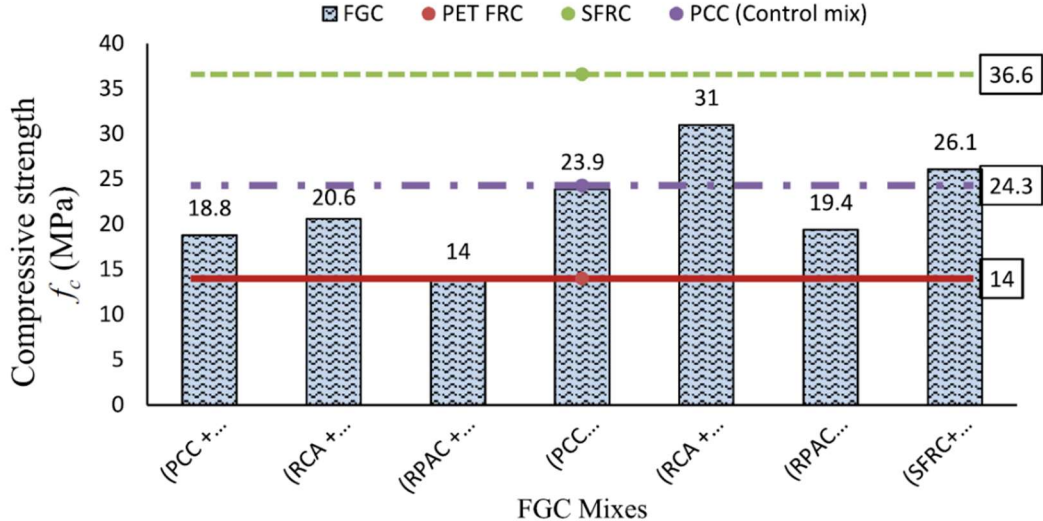


Figure 15 Compressive strength comparison of PET-FRC, SFRC, and FGC mixes. [14]

Chapter 3

Second life fibers from end life tires

3.1 Recycled steel fibers (RSF)

RSF refers to the high-strength steel fibers reclaimed from shredded tires during the recycling process.[15], [16], [17] Tires contain embedded steel wire reinforcements, which are separated during recycling, cleaned, and repurposed as reinforcing fibers for concrete.[16] RSF retains the high tensile strength (generally >800 MPa) of the original steel used in tires and thus becomes a suitable candidate for concrete reinforcement. Though recycled, RSF usually retains good ductility that helps in bridging of cracks in concrete. RSF is typically produced with hooked or curved ends depending on the extraction process. These shapes may enhance anchorage and bonding with the concrete matrix. Provides a second life for materials bound for landfill disposal, thus helping significantly reduce environmental impacts.



Figure 16 dirty fibers on the left, cleaned final fibers on the right

The fibers that come out from industrial recycling of end life tires have still 2% of dirty, in that condition they could not be used for structural purposes, that is why they undergo another

cleaning process where almost of the dirty from the tires is removed and now they can be applied to a cementitious matrix.

3.2. Fibers from AGR Torino

The fibers used for my case study comes from AGR TECH company in Cumiana(TO), this industry recycles end life tires and transforms the recycled product in second life technologies. Approximately 5 kilograms of fibers were received and taken under study. The studies were done to evaluate the characteristics of the fibers, geometry and which is the most suitable mix design to use the RSF to obtain the maximum results and benefits, trying to verify the effectiveness of the structural performance, compared to industrial fibers.



Figure 17 steel fibres from AGR

3.2.1. Statistics

From the fibers received, a sample was extracted from it to do a statistical analysis, over 430 fibers were measured with an electronic caliber, the diameter and the length of each fiber with also their shape, here reported the results obtained from MATLAB.

The range refers to the difference between the maximum and minimum values in a dataset. It gives a sense of how spread out the data values are.[18] The value of range_L is 49.3. This indicates that the difference between the largest and smallest values in the dataset for L is:

$$Range_L = L_{max} - L_{min} = 49.3 \quad (3.1)$$

While the range provides a quick idea of variability, it only considers the extremes and does not account for the distribution of the rest of the data.

The mean (average) is the sum of all the data points divided by the number of data points. It represents the central value of the dataset.[18] Mean_L = 22.92: This is the average of all the L values in the dataset. On the other hand the standard deviation measures the amount of variation or dispersion in a dataset. [18] A higher standard deviation indicates that the data points are more spread out from the mean, while a lower standard deviation indicates that they are closer to the mean.[18]

The value of std_L = 7.8517. This means that the L values typically deviate by about 7.85 from the mean value.

In conclusion, the median is the middle value of a dataset when it is ordered from smallest to largest. If the dataset has an even number of values, the median is the average of the two middle numbers.[18]

The value of the median_L is 22. This indicates that half of the L values are below 22, and half are above 22.

Here below are reported the statistics data collected for the length of the fibers measured, comments will be follow the tables.

Table 5 statistic for L

Statistic	Meaning	Value
mean_L	The average value of L.	22.92
std_L	The standard deviation (spread of L).	7.8517
median_L	The middle value of L (central value).	22
range_L	The difference between the max and min L.	49.3

The same process was done for the diameter D:

Table 6 statistics for D

Statistic	Meaning	Value
mean_D	The average value of D.	0.28885
std_D	The standard deviation (spread of D).	0.15545
median_D	The middle value of D (central value).	0.28
range_D	The difference between the max and min D.	1.49

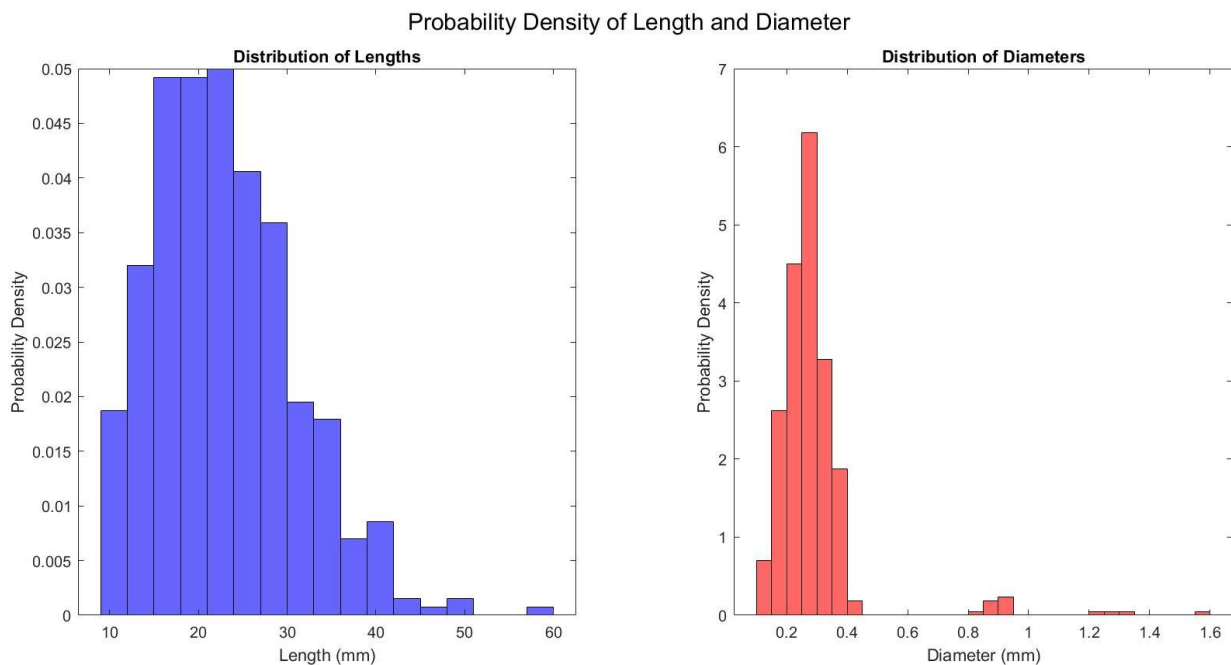


Figure 18 probability density plot for length(a), and diameter of fibers(b)

In the left plot the distribution is almost normally shaped but somewhat skewed toward shorter lengths, with a long tail extending to the right. The peak density is at around 20–30 mm, indicating that the majority of fibers would likely fall in that general range in length. Spread out, there is an observable distribution from some 10 mm to as high as 60 mm. Although when judging from the myriad values presented above 40 mm, such lengths do seem to be rare. There are very few instances above 50 mm, indicating that in this data set, longer fibers seem to be uncommon.

The diameter distribution is highly skewed toward the right. Most of the values crowd at the lower end of the diameter spectrum (0.2-0.4 mm). The maximal density lies at approximately 0.3-0.4 mm, which means the majority of fibers fall under this diameter. This distribution has a much more narrowed spread, where most values fall between 0.2 mm and 0.6 mm; a few, however, extend up to 1.6 mm, suggesting the presence of rare, thick fibers. With very few fibers found to record a diameter greater than 1.0 mm, it indicates that these are either outlier cases or special cases.

To make a comparison between the two plots, the length distribution show wider spread as compared to diameter distribution, which was more concentrated from close small range. These distributions are critical because the lengths and diameters both contributed to the strength imparting characteristics of the material such as bridging the cracks in longer fibers, while smaller diameters increase the surface area available for bonding with the matrix.

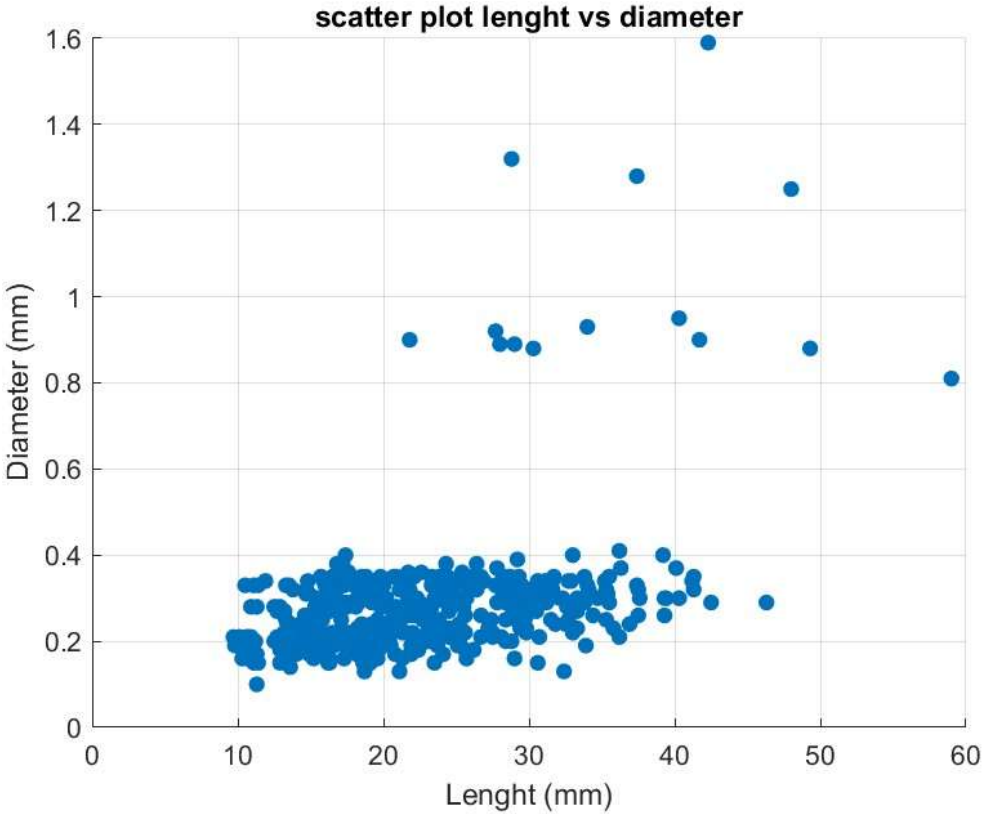


Figure 19 scatter plot length vs diameter

Hence, the scatterplot is capable of representing the whole variance explained by the data. Given that the majority of the fibers are in the regions of smaller diameters and shorter

lengths, there are crucially important outliers that show trends in higher diameters and maximum lengths. These deviations may be crucial in understanding the material properties and in modifying the applications in fiber-reinforced composites.

Aspect Ratio for Fibers:

1. Definition:

$$AR = \frac{L}{D} \quad [5] \quad (3.2)$$

-For fibers, this ratio indicates how long and thin the fibers are compared to their diameter.

With the increase of aspect ratio some effects take place in the FRM or FRC product, in fact, the workability decreases, structural performance generally increases, for what regards compression there is no direct correlation, instead for flexural strength there is a great benefit, as well as the tensile strength and the reduction in permeability of the concrete, which might give a better durability.[19]

Table 7 AR statistics

Statistic	Meaning	Value
mean_AR	The average value of AR.	86.38
std_AR	The standard deviation (spread of AR).	30.85
median_AR	The middle value of AR (central value).	82.85
range_AR	The difference between the max and min AR.	41.82

Some comments about the shape of these RSF, recycled fibers may have different shapes, the ones of the discussed case study were almost all wavy and hooked, a negligible percentage was of other different shapes.

Especially when it comes to hooked fibers, clear improvements are seen in flexural strength, as well as when adding an higher volume of fibers. [19]

3.2. Fitting For Length, Diameter and Aspect Ratio

The data collected have been studied how they fit in three different distribution models:

- Normal: Assumes data are symmetric and bell-shaped around the mean. [20]
- Lognormal: Suitable for datasets with positive skewness, if the distribution of logarithm of the variable values follows a normal distribution. [20]
- Weibull: Commonly used in reliability and lifetime analyses[20]

3.2.1. Qualitative analysis of distributions fitting

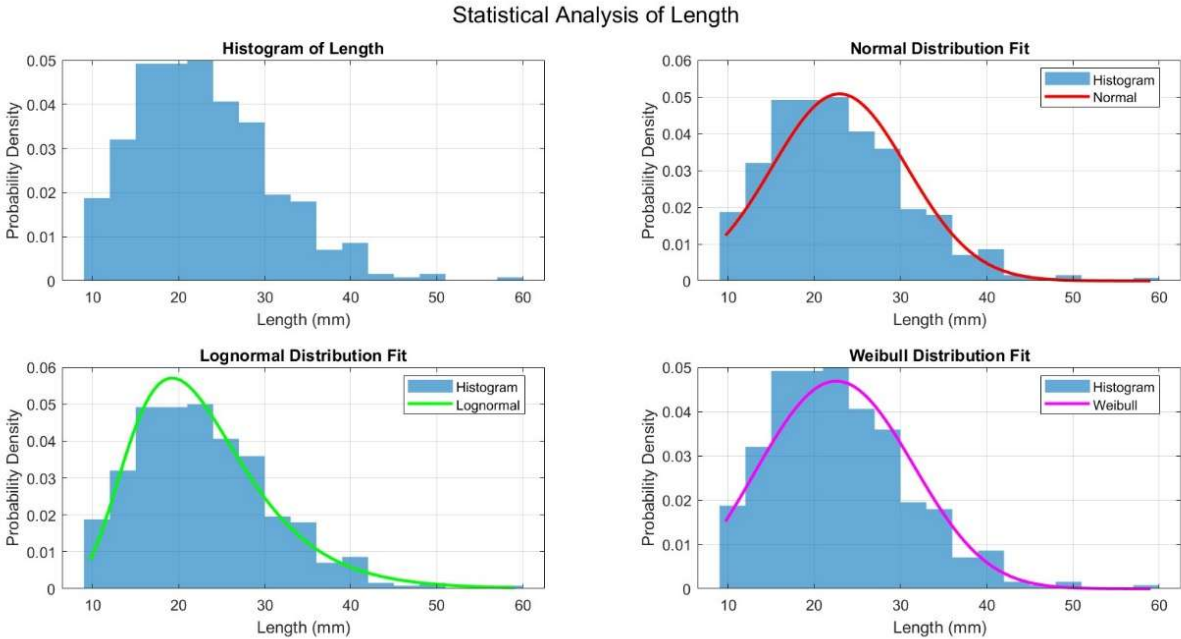


Figure 20 fit distribution length of fibers

The red curve represents a normal curve to the given data set.

Note that the normal curve appears to fit the histogram moderately around the center but does not seem to accommodate the actual skew in the data very well.

As we expect in any dataset, a normal distribution appears to be symmetrical, but the data skews to the right – putting the normal distribution model at a disadvantage because it is ill-fitted on this specific dataset.

A lognormal distribution has been fitted to the data as well and is represented by the green curve. There seems to be a reasonable concurrence between the lognormal and the histogram distribution, particularly as it concerns the negative skewness of the data.

Since non-negative values are assumed, the right-skewed lognormal distribution is more representative in this case than the normal distribution.

The Weibull distribution fitted to the data set is shown by a magenta curve.

The Weibull distribution fits the data reasonably well, particularly for the upper peak and right tail of the histogram.

In many cases, Weibull distributions are employed in reliability analysis because this type of distribution can accommodate skewed data like this.

Statistical Analysis of Diameter

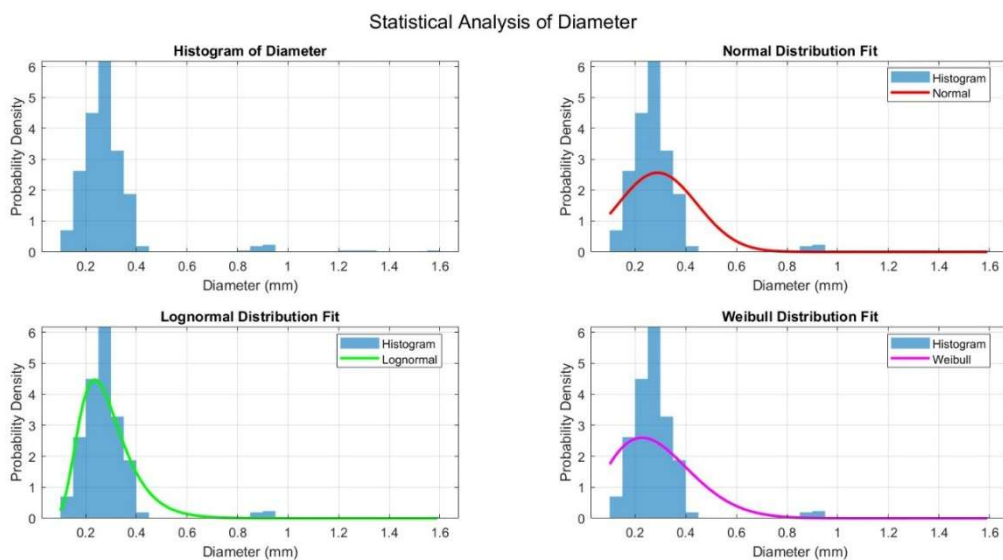


Figure 21 fit distribution for diameter of fibers

Lognormal distribution can do better for fitting to the skewness than the normal distribution.

It provides a good fit for the bulk of them lying between 0.2 mm and 0.5 mm and is characterized by a long tail.

The magenta line represents a Weibull fit.

The Weibull distribution renders an almost similar fit to that of the lognormal distribution, although slightly biased toward the center.

Statistical Analysis of Aspect Ratio (L/D)

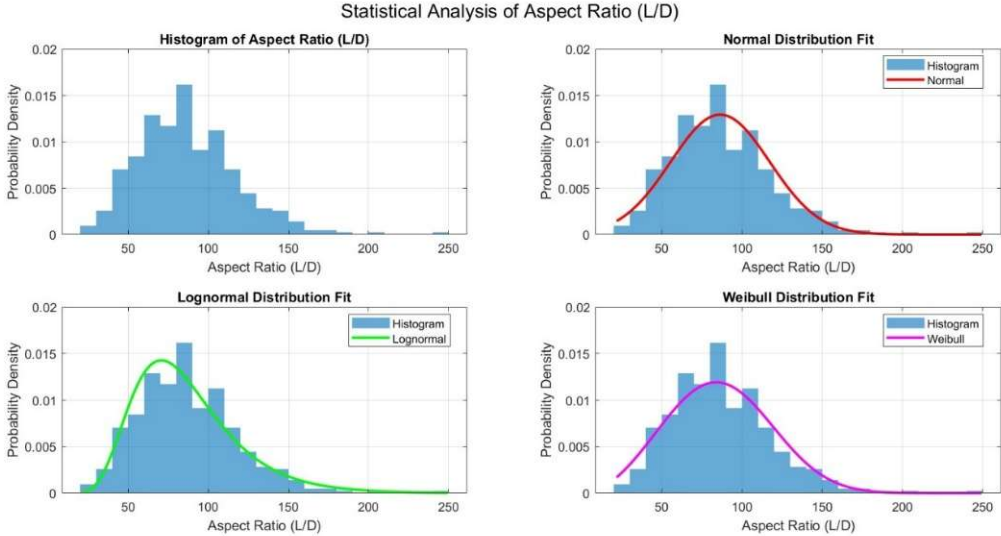


Figure 22 fit distribution for aspect ratio of fibers

This histogram shows the probability density of the fiber aspect ratio (length/diameter). Most aspect ratios lie between 50 and 150, with a peak near 100. The distribution is relatively symmetric, with a few higher aspect ratios, extending up to 250. The red line indicates the normal distribution fit over the histogram data. For most of the areas of interest, it describes an adequate representation of the main population; thus, the box was unnoticed with any extreme values. The green line represents a lognormal fit. The lognormal distribution captures the slight skew in the data better than the normal distribution. It fits well for the concentration of values between 50 and 150 while accounting for higher aspect ratios. The magenta line here represents a Weibull fit. The Weibull fit looks very close to the normal distribution behaviour.

3.2.2. Goodness of fit tests

To verify effectively which of the chosen distributions fit best with the data, it is necessary to do a quantitative analysis through some tests. Such process is called goodness of fit tests, and for the collected data there will be used two specific tests, Anderson Darlin test and Pearson test, also known as Chi Squared test. The goodness of fit of the described models, has the purpose to evaluate the discrepancy between the observed values and the values expected under a statistical model. [21] The Anderson Darling test is used to test if a sample of data came from a population with a specific distribution, it gives more importance to the tails of the distribution and has critical values to be estimated, which are used to evaluate the results[22]. Coupled with

the Anderson Darling test , there is the Pearson test, the chi-square goodness-of-fit test is used to determine whether a sample aligns with a population that follows a specified distribution.

Essentially, it assesses whether the observed frequency distribution matches an expected or hypothesized pattern. [22]

Table 8 goodness of fit tests

Goodness of fit tests	Normal	Lognormal	Weibull
AD Hypothesis[L]	1	0	1
AD p-value [L]	0.0005	0.0858	0.0005
Pearson(Chi-Squared Hypothesis)[L]	1	0	1
Pearson(Chi-Squared)pvalue[L]	0.0002	0.6810	0.0011
AD Hypothesis[D]	1	1	1
AD p-value [D]	0.0005	0.0005	0.0005
Pearson(Chi-Squared Hypothesis)[D]	1	1	1
Pearson(Chi-Squared)pvalue[D]	0.0000	0.0000	0.0000
AD Hypothesis[AR]	1	1	1
AD p-value [AR]	0.0005	0.0041	0.0005
Pearson(Chi-Squared Hypothesis)[AR]	1	0	1
Pearson(Chi-Squared)pvalue[AR]	0.0019	0.4198	0.0020

The parameters considered to evaluate if the datasets of length, diameter and aspect ratio follow a specific distribution are:

h (Hypothesis Test Result)

- $h = 0$: Fails to reject the null hypothesis → The data fits the given distribution. [23]
- $h = 1$: Rejects the null hypothesis → The data does not fit the given distribution.[23]

p (p-value)

- The p-value indicates the probability that the observed data could come from the specified distribution. [23]
- A higher p-value suggests a better fit. [23]
- If $p < \alpha$ (usually $\alpha = 0.05$), the fit is poor, and we reject the distribution. [23]

Based on the results reported in the table 8, the only distribution which passes both Anderson Darling and Pearson tests is the lognormal one, but this happens only for the L datasets, while for diameter and aspect ratio datasets it is not.

The plots and the results described in the chapter 3 were all obtained through a code in MATLAB reported in the ‘Appendix A ‘.

Chapter 4

Experimental analysis

4.1. Mix design

To verify effectively if the fibers have a positive impact in terms of structural performance, they have to be mixed in a mortar and then study how the reinforced fiber material behaves under loads. First, a mix design is necessary to set all the required steps in order to obtain the best from the final product.

The purpose of a mix design is to choose the most appropriate components, as well as proportions to get the best results from the final product[24], which is in this case an FRM. Such processes start from defining the requirements, which are the expected values of resistance which the material should achieve under bending and compression. Then it continues by selecting cement, water, fibers and fine aggregates to produce an economic mix with the required fresh and hardened properties.[24] The proportions might change based on the requirements or the relevant standards, which are important for each material involved in the mix design (ASTM, ISO, etc.). The process of achieving the right combination of cement, aggregates, water, and admixtures is called mix proportioning or mix design. [24]

What Constitutes a Mix Design:

1. Cement-Brings the mix together as a binder.
2. Aggregates-Take space and keep the shrinkage down. Fine aggregates (sand) only in mortar; in concrete, both fine and coarse aggregates are present.
3. Water-Hydrates the cement and makes it workable.
4. Admixtures-Optional: Any extra material that is put to change properties (Superplasticizers for workability; Air-entraining agent for freeze-thaw resistance).
5. Reinforcement Fibers-Steel, glass, or polypropylene fibers might be added to increase resistance to cracking and to impart tensile strength. In this case study the mix design was planned based on two reinforcement index and two types of steel fibers, one type is industrial(fixed characteristics), the other one is from end-of-life tires (RSF).

Table 9 fiber types and their volume

Fiber Type	Average L/D Ratio	Average Length	Average Diameter (D medio)	RI	Vf
Recycled Fibers	86	23 mm	0.29 mm	40%	0.47%
				60%	0.70%
Industrial Fibers	50	20 mm	0.4 mm	40%	0.80%
				60%	1.20%

RI (Reinforcement Index):

The Reinforcement Index (RI) is a measure of the percentage of reinforcement fibers in the mix relative to other components. It quantifies how much fiber is present as a reinforcement in the composite material. A higher RI typically means more fibers are used to strengthen the material. [25]

V_f(Fiber Volume Fraction):

The Fiber Volume Fraction (V_f) represents the percentage of the total volume of the material that is occupied by fibers. It indicates the proportion of fibers in the composite mix by volume, which directly affects the strength, stiffness, and toughness of the composite. [25]

Formula for V_f:

$$V_f = \frac{AR}{RI} \quad (4.1)$$

$$V_f = \frac{V_{fibers}}{V_{total}} * 100 \quad (4.2)$$

- V_{fibers} = Volume of fibers
- V_{total} = Total volume of the mixture
- AR = aspect ratio

- RI= reinforcement index
- If $V_f = 0.47\%$, only 0.47% of the composite's volume is occupied by fibers.

Now let's define the amount of the materials to use for the mortar samples, the aim is to realize a total number of 15 samples:

- Three samples of reference material without reinforcement
- Three samples of reinforced mortar with an RI of 40% and fibers from end-of-life tires
- Three samples of reinforced mortar with an RI of 40% and industrial fibers
- Three samples of reinforced mortar with an RI of 60% and fibers from end-of-life tires
- Three samples of reinforced mortar with an RI of 60% and industrial fibers

Table 10 mix design quantities

	CEM II	sand	water	fiber Rec.	Ind. fiber	superplasticizer
mortar	(g)	(g)	(g)	(g)	(g)	(g)
ref	450	1350	225	0	0	0
R_40	450	1350	225	36.5	0	4.5
I_40	450	1350	225	0	62.8	4.5
R_60	450	1350	225	54.8	0	4.5
I_60	450	1350	225	0	94.2	4.5

Cement is a fixed amount based on the desired **binder content** for the mortar mix. It reflects the standard proportion for a typical mortar mix where the ratio is:

- Cement:Sand = 1:3 (by weight)

Since sand is 1350 g (3 parts), the cement (1 part) is calculated as: $\text{Cement/sand} = 450\text{g}$

Sand is three times the weight of cement in this mix. This 1:3 ratio ensures adequate workability and strength for mortars.

The water content is determined based on the water-to-cement ratio (W/C ratio), which typically ranges from 0.45 to 0.50 for mortars.[26]

- Given a water-to-cement ratio of **0.5**, the water is calculated as:

$$450\text{g} * 0.5 = 225\text{g} \quad (4.3)$$

Superplasticizers are typically dosed as a percentage of the weight of cement, depending on the specific type and manufacturer's recommendation. The dosage range given by the product is 0.5%–1.5% of the cement weight. For this case it is fine since it is a type II cement.

Calculation:

- Cement weight = 450 g
- Superplasticizer dosage: 1% of cement weight

$$d_{\text{superplasticizers}} = m_{\text{cement}} * \frac{1}{100} = 450g * 0.01 = 4.5g \quad (4.4)$$

4.2. Samples preparation

Since the mix design has been done, the process of samples preparation can start

All the ingredients are measured using an electronic balance for any discrepancies in accuracy of the measurement.

Cement: 450 g (constant for all samples in your case).

Sand: 1350 g standard sand weighing as represented in the first image.

Water: 225g (constant for all mixes unless otherwise stated).

- For R_40, 36.5 g of recycled fibers ($V_f = 0.47\%$).
- For I_40, 62.8 g of industrial fibers ($V_f = 0.80\%$).
- For R_60: Recycled fibers 54.8 g ($V_f = 0.70\%$)
- For I_60: Industrial fibers 94.2 g ($V_f = 1.20\%$)
- Superplasticizer: Fixed at 4.5 g in the mix designs.
- Fibers can be pre-weighed and set aside in containers to avoid delays during the mixing process.

Automatic mortar mixer.

Setup:

- Fix the mixing bowl tightly.
- Clean paddle and set it up correctly.
- Set the standard mixing procedure, that is, EN 196-1. [27]



Figure 23 mixer

Cement and sand are the measured quantities put in the mixer.

Starting at a low speed, the mixer continues for 30 seconds to ensure distribution of dry materials uniformly. [27]

While running at low speed, the pre-measured water is poured slowly into the mixing bowl.

Mixing continues for one minute after adding all the water.[27]

Add fibers slowly (both recycled and industrial) to the mixer while in operation. They should be added in small amounts to avoid clumping.

Let the mixer run for 1 minute to be able to ensure that the fibers are uniformly distributed within the mix.[27]

Two types of fibers were used, the ones produced from industry and the others, extracted from shredded end-of-life tires.



Figure 25 RSF from end-of-life tires



Figure 24 industrial fibers

Add the pre-measured superplasticizer.

Continue mixing for 1 more minute at medium speed. The mix should appear homogeneous, with no fiber clumps or segregation.[27]

The superplasticizer made the process much easier, since fiber mixing could give some issues to the mixer, but no problem arose at all.[27]

Now the moulds are prepared



Figure 26 moulds oiled

Assemble the molds on the compaction/vibration table, ensuring they are tightly secured to avoid leaks.

The moulds are oiled before filling them with mortar to ensure a smooth and easy demoulding process after the mortar hardens.[27] [28]Here are the key reasons:

Oiling the moulds prevents the mortar from sticking to the mould,[28] moreover it might help to achieve a cleaner and smoother surface of the sample at the end of the curing process, avoiding damages and potentially having a better performance during structural tests. [27]

Pour the freshly mixed mortar into the molds, filling them to about halfway, then it can be used a tamping rod or gentle vibration to remove any trapped air bubbles. Add the remaining mortar to fill the molds completely. Again, use tamping or vibration to ensure uniform compaction.[27][28]



Figure 27 filled molds with mortar

Through the use of the machine level-surface, mount molds and machine and complete surface leveling. The repeats of stuffing allow improved density of the mix as excessive air bubbles are struck out of it. It helps to flat the surface and spread compaction uniformly.

In effect, this gets a damp cloth placed over the molds immediately to retain moisture after evaporation is halted. The mortar was left to cure for 24 hours in a controlled atmosphere ($20\pm 2^\circ\text{C}$, 95%RH if possible). [27]

Molds are checked in a day or two; inspection of concrete bricks is done at this point.

Place the newly detached samples in the curing chamber or water bath maintained at $20 \pm 2^\circ\text{C}$. [27]

Water curing can go for 7 or 28 days; again test method says how much longer must they be stored in their curing environment. [27]

This explained approach ensures consistent and quality sample preparation and can be retested errorless. This detailed approach ensures consistent and high-quality sample preparation, suitable for reliable experimental testing.

4.3. Tests

At the end of the curing period, samples are ready to be taken out from the molds and tested to check the structural performance, the tests that were done are two:

-3 points bending test

-Compression test

To give a better understanding of what was mentioned, the 3-point bending test is a common mechanical test used to evaluate the flexural properties of materials, such as beams or joists, by applying a force at the center while supporting the sample at two ends. [29] If the joist fails in this test, the broken pieces can further be tested under compression to assess the material's compressive properties. This test aims to determine the flexural strength, as well as the stiffness and behavior of a joist or beam under bending stress. [29] The joist (or beam sample) is placed horizontally on two support points (span). A force (load) is applied vertically at the midpoint of the joist until it breaks. [29] As the load increases, the bottom of the beam undergoes tensile stress, while the top experiences compressive stress. [30]

When the tensile stress exceeds the concrete's strength, micro-cracks form at the bottom and propagate upward. In FRC, the fibers within the concrete bridge the cracks and hold the structure together, delaying complete failure. The purpose of this test is to determine:

The load-deflection data can be used to calculate:

Maximum load before failure, which is the flexural strength (resistance to bending) [29]

Modulus of elasticity (how much the joist bends under load)[29]

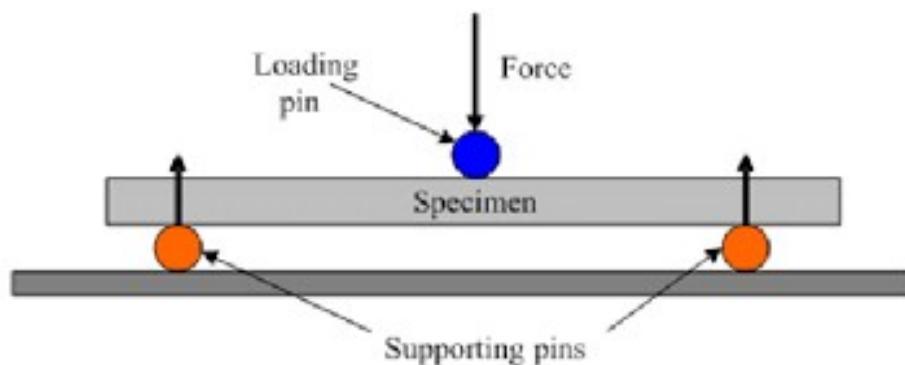


Figure 28 3-point bending test scheme

Compression Testing:

A vertical force is applied to compress the material until failure or deformation occurs.[31]

First of all, the specimen is positioned to have a uniform loading where it is compressed between two plates.[31]

With the chosen rate of loading, it is applied a compressive force, which will stop till failure of the specimen. [31]

Continuously record the load (force) and the corresponding displacement or deformation throughout the test.[31]

In FRC, the fibers within the mortar help to strengthen the sample and delay the failure, even though the fibers have more benefits in terms of bending, the reinforcement resulted to give a better performance. This test has the purpose to:

To determine compressive strength (the maximum stress the material can withstand under compression).

To analyze whether failure was due to material weaknesses (e.g., fibers crushed or buckled under bending).

To gather additional data on material performance in different stress conditions.

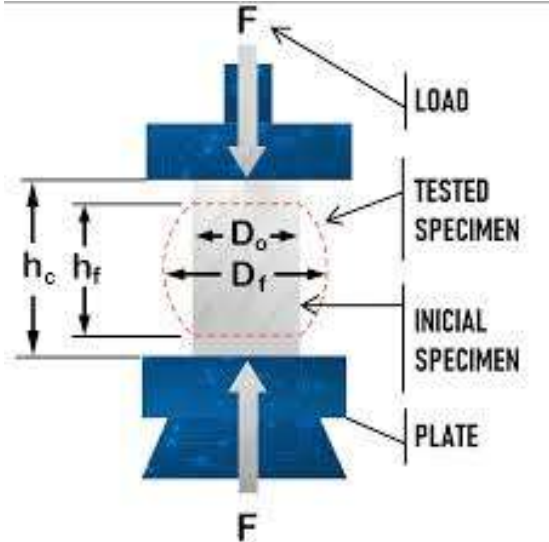


Figure 29 compression test scheme [31]

In the picture above, the specimen is cylindrical, but for our case study it is a beam. Combining these two tests, the material characterization is basically complete, the law requirements are fulfilled and a general overview of this technology’s strength can be easily obtained, without no further testing.

Table 11 plain and FRC response under loadings

Property	Plain Concrete	Fiber-Reinforced Concrete
Failure in Bending	Sudden, brittle fracture	Gradual, post-crack resistance
Flexural Strength	Lower	Higher due to fiber bridging
Toughness	Low	High, improved energy dissipation
Compressive Strength	Brittle failure	Delayed, gradual failure
Ductility	Low	High, due to crack control

Chapter 5

Results

5.1. Three point bending and compression test results

The Lab of Polito has provided both the testing machines for the above purposes; after removing the samples from the baths where they have been curing, the tests are ready to be performed, such tests are going to evaluate the peak values that will be used later to estimate the resistances.



Figure 30 samples after 28 days of curing

In the picture above the samples after 28 days of curing are shown, as a reminder of what previously mentioned, three are of reference, so without any reinforcement, while the others are reinforced with two different RI, and both industrial and recycled fibers, the tests might determine what are the positive effects of the fibers and how much beneficial are to the cementitious matrix.

A large improvement in terms of peak load and eventually of resistance, first for bending and later in compression, is expected to be shown in the curves reported from the testing machines, hopefully with reasonable behaviors.

In the case of non-reinforced beams the failure is not well shown, it is necessary to zoom very close to the crack to clearly see it.

5.1.1. Calibration of the machine and measurements of the samples

The distance between these two lower supports was set at 10 cm (100 mm) for support span.

The supports were symmetrically aligned, according to the condition for the typical beam of perfect stability and uniform loading.

Beam dimensions are approximately $40 \times 40 \times 160$ mm.

The beam length is longer than support span, keeping sufficient overhang for securing results.

The load was applied at a distance of approximately 8 cm from each support at the mid span; this results in a central loading condition.

The machine applies the force through a single-point loading head, which is clearly seen pressing down on the beam's center.

Force application is gradual, to produce bending and record the peak force and deflection before failure.

The real dimensions of the beams were measured with an electronic caliper and recorded to be assigned on the machine before the starting of the test, as well as the weight, the marks reported on the beam are to facilitate the positioning of the beam, two marks on the side at 3cm distance from the edge, and one in the middle at 8cm where the load is applied.

For what regards the geometric properties there is a very small variation, with values ranging from from 39 to a max of 42mm, even less variation are noticed in the height of the samples and in the length. Such variation might be due to imperfection during the molding process, and compaction.

On the other hand, the reinforcement shows high benefits in terms of resistance in both bending and compression, especially when the amount of fibers is higher, with an RI of 60%, trends demonstrate how crucial is for mortar and concrete to have a reinforcement which is properly mixed into the matrix. Furthermore, some samples show constant trend of values, which is representative of good quality process. All of this is reported in the table below.

Table 12 measured sample characteristics and geometry

Sample ID	B (mm)	H (mm)	Peso (g)	Length (mm)	Pmax (N) Bending	PA(N) Compression
REF_1	39.18	39.83	572	159.9	1660	$9.24 \cdot 10^4$
REF_2	40.60	39.90	584	159.9	1800	$9.68 \cdot 10^4$
REF_3	40.875	39.97	582	160.0	1960	$9.18 \cdot 10^4$
R40_1	40.33	39.72	596	160.5	2780	$1.19 \cdot 10^5$
R40_2	39.47	40.00	587	160.1	2060	$1.10 \cdot 10^5$
R40_3	40.63	39.95	591	160.1	2750	$1.18 \cdot 10^5$
I40_1	40.60	39.96	587	160.4	2750	$1.06 \cdot 10^5$
I40_2	39.60	39.97	586	160.2	2750	$1.06 \cdot 10^5$
I40_3	40.35	40.17	605	160.4	2570	$1.12 \cdot 10^5$
R60_1	41.50	39.93	601	160.4	3840	$1.05 \cdot 10^5$
R60_2	41.62	39.24	596	160.4	3060	$1.05 \cdot 10^5$
R60_3	42.50	40.11	600	159.7	3720	$1.05 \cdot 10^5$
I60_1	41.09	40.00	599	160.1	2810	$1.14 \cdot 10^5$
I60_2	41.75	40.44	611	160.1	3820	$1.09 \cdot 10^5$
I60_3	42.38	40.00	610	160.2	4590	$1.12 \cdot 10^5$

5.1.2 Testing of the samples and failure study

It is appropriate to have a better understanding of how the samples behave during both the bending and compression tests, because the failure mode gives insights and clear information of the quality of the product that was produced and how good was the mix design and molding of each sample.

Three cases are reported below, samples without reinforcement, with RSF reinforcement and industrial fibers reinforcement.

Reference samples with no reinforcement:



Figure 32 Ref_1 sample before the test



Figure 31 Ref_1 sample after failure

Now let's see how RSF fibers behave:

As it was described before, in the other 12 samples, there were added fibers, both recycled and industrial, in the next pictures it will be shown, as it has been done for the references samples, how the beams behave under bending test, the way they brake and how good and beneficial is the fiber effect on the mortar.

It is expected that there will be a more ductile behavior with a more delayed failure and higher peak load, resembling an higher performance.



Figure 34 R40_1 sample before testing



Figure 33 R40_1 sample after failure

Finally industrial fibers behaviours:



Figure 36 I40_1 sample before testing



Figure 35 I40_1 sample at failure

When fibers are added , the failure behaviour is much more evident and demonstrates the ductility effect and benefits of steel into the structural mortar, these benefits might also be seen in the peak load increase and longer time of testing before cracking. On the other hand, the reference samples show a brittle failure, with a sudden cracking, and the failure crack is almost not visible, nevertheless, not all samples gave better structural performance compared to the not reinforced beams

5.1.3. Curves force-displacement

The test provides and plot force-deflection curve (or load-displacement curve), which are used to study how the procedure of loading evolves in time, here below are reported the curves of the samples previously shown:

Y-axis (Standard Force, N):

This represents the applied load on the specimen, measured in newtons (N). As the load increases the curve starts to rise more and more.

X-axis (Standard Travel, mm):

This is the deflection or displacement of the specimen at the midspan, measured in millimeters (mm). It is an indicator of how much the sample bends and moves downward under the progressive loading

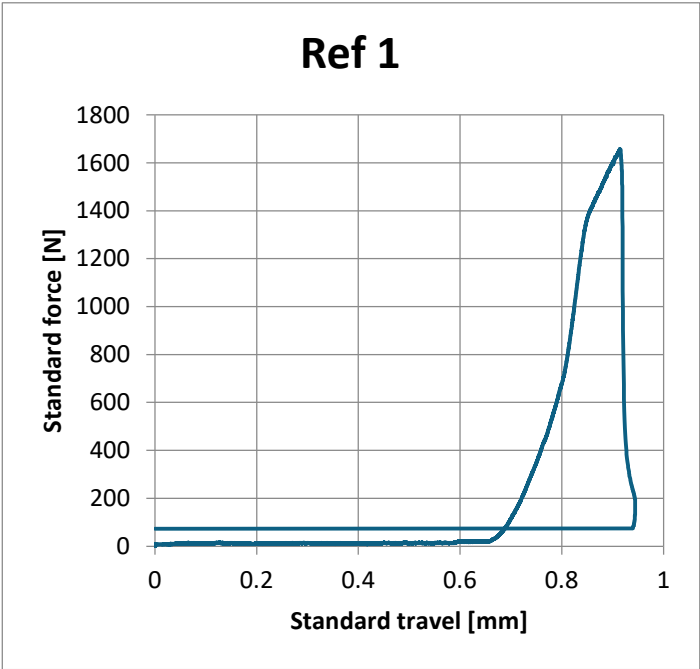


Figure 37 Ref_1 force-displacement curve (bending test)

The curve starts with a nearly horizontal segment up to about 0.4 mm.

This indicates the material was undergoing minimal deformation under low force. It might represent the alignment or seating of the specimen or a phase where the material is still within a very low strain range.

Steep Linear Region:

- After about 0.4 mm, the curve rises steeply.
- Elastic phase: The material elongates further in strict proportion to the applied force.
- Determining the slope in this region can give an insight into the stiffness or modulus of elasticity of the material.

Peak Force:

- At around 0.9 mm deflection, the curve peaks at about 1800 N.
- Here, failure or the maximum capacity load of the material is reached.

Sharp Drop:

- After the peak, the force drops off quickly, signaling material failure.
- Were this a brittle failure, it would mean a quick drop without much remaining capacity.

Recycled fibers behaviour:

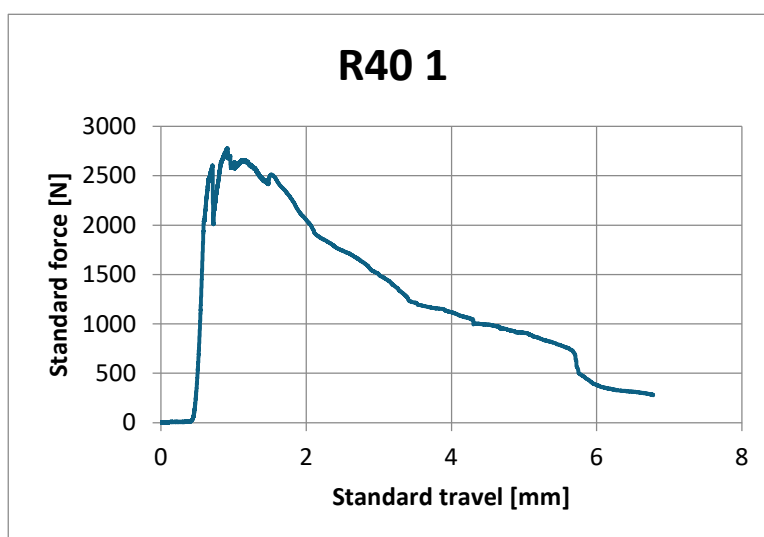


Figure 38 R40_1 force-displacement curve (bending test)

The initial sharp rise corresponds to the **elastic region**, where the material deforms elastically (linear region). The **peak load** (around 2700 N) represents the maximum force the material can withstand before cracking occurs. The subsequent decline indicates **post-crack behavior**,

where the fibers (steel fibers in this case) bridge the crack and provide residual strength as the deflection increases.

Industrial fibers behaviour:

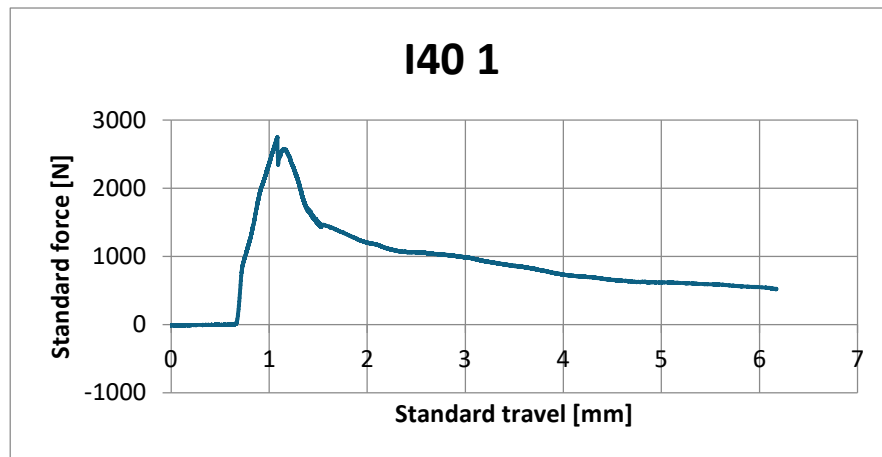


Figure 39 I40_1 force-displacement curve (bending test)

The curve commences at zero and climbs steeply, designating elastic deformation of the material. That was the linear elastic phase where the material follows Hook's law.

The curve reaches the ultimate force, representing the utmost load-bearing capacity of the specimen. This indicates the creation of lesions or cracks in the material.

A rapid drop of applied force after the peak indicates propagation of the cracks or a sudden drop of stiffness. This is the stage where matrix cracking generally occurs for fiber-reinforced concrete (FRC).

The force gradually decreases with an increase in displacement, indicating the participation of fibers in bridging the cracks.

The curve plotting stops at its tail's end where the sample is at complete failure, what this curve has shown is a very clear post-cracking ductility provided by the steel fibers.

Compression:

The sample split in two parts, one part was used for the compression test, the other one for further researches and studies, now we go into deep study of the compression study. The machine is equipped with a loading plate (circular plate at the top) that applies a compressive

force on the fractured specimen. The crossbar securely holds the small, broken sample in



Figure 40 Ref_1 sample before testing



Figure 41 Ref_1 after failure

place, this apparatus is made for this type of sample with the dimension previously described, this facilitates a uniform loading.

Materials like plain concrete or mortar, when subjected to compressive loads, exhibit a brittle failure mechanism.[4] Once the load exceeds the material's compressive strength, cracks propagate rapidly without any reinforcement that slows down the failure process. This leads to an explosive failure, characterized by a sudden fractures of the sample in broken pieces.[4]

Now with reinforced samples:



Figure 43 R40_1 sample before testing



Figure 42 R40_1 after failure

As compressive load increases, fibers help to bridge the cracks and hold the material together, redistribute stresses around micro-cracks, thereby delaying their growth and propagation, and help to absorb energy so that the material deforms more slowly rather than failing catastrophically. [4] Hence, the fiber-reinforced specimens generally exhibit less violent failure, showing comparatively gradual crushing with limited fragmentation. The same behavior is observed with the industrial fibers.

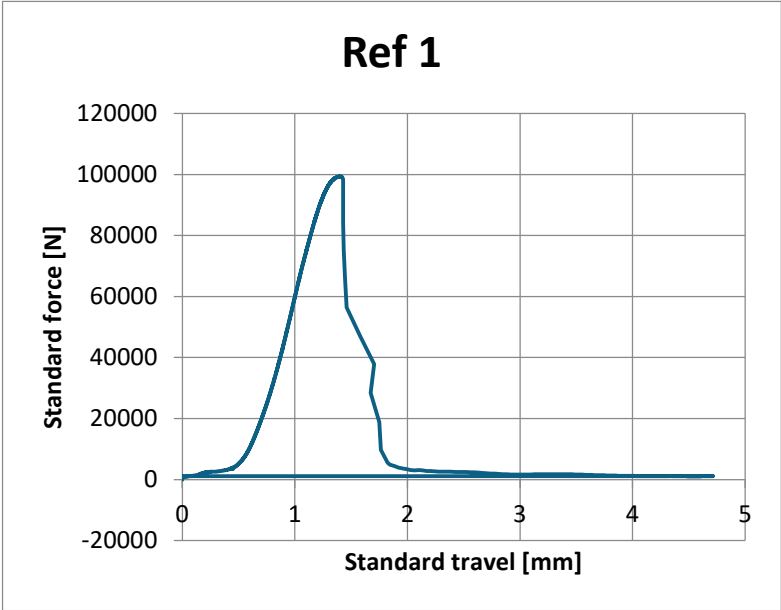


Figure 44 Ref_1 force-displacement curve (compression test)

The peak force occurs at approximately 100 kN (or 99,392N as earlier given), after which, the behavior is sudden and explosive, characterized by a sharp drop on the force-displacement curve.

The referenced specimen demonstrates a brittle failure mode one would expect of plain concrete under compression.

Once maximum compressive strength is exceeded, the specimen shows a rapid fall in load-bearing capacity with a steep drop in the post-peak curve. Ref_1 Exhibits the lowest peak force and compressive strength in line with the expectation of intense brittleness and limited load-carrying capacity offered by plain mortar.

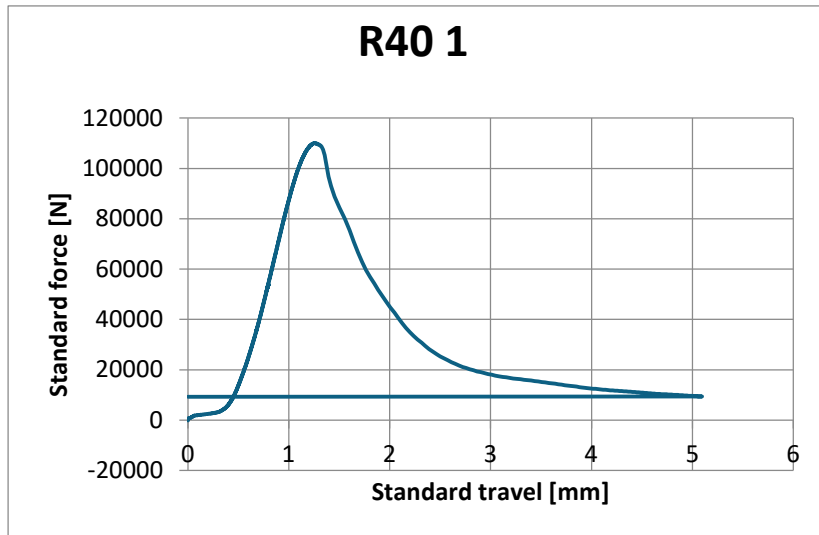


Figure 45 R40_1 force-displacement curve (compression test)

Around 110,194 N (about 110,000 N) is the maximum force, which is higher compared to Ref_1; this reinforces the idea that the compressive strength increases due to recycled fibers. After the peak force, the curve descends with less slope than Ref 1, which suggests greater ductility. Such behavior indicates that recycled fibers cause better energy absorption and retard the collapse of the specimen.

The R40_1 sample shows a heavy improvement in compressive strength due to the recycled fibers, and about a 10% rise in maximum resistance, reducing the brittle failure.

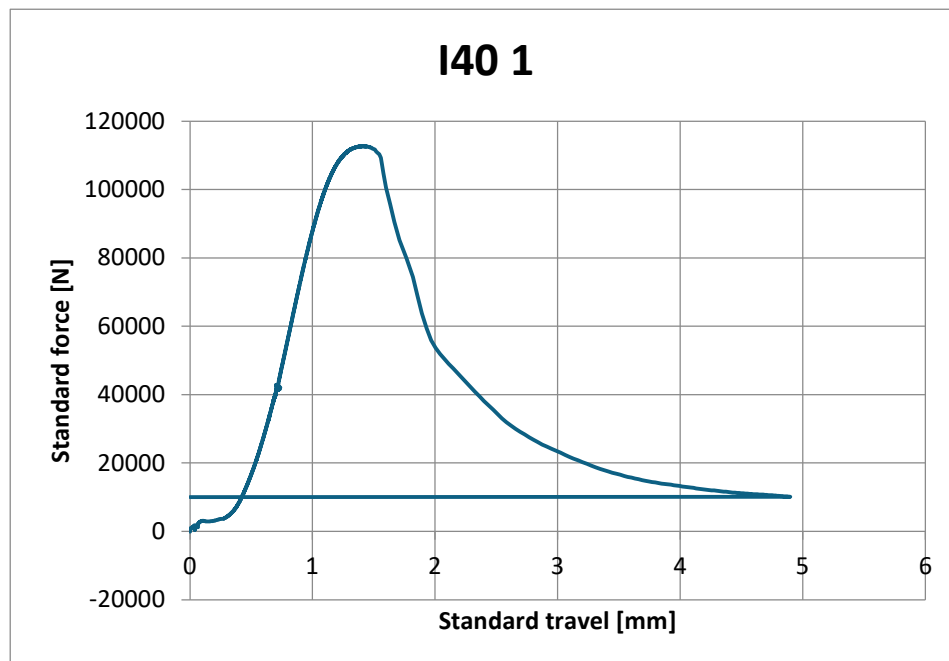


Figure 46 I40_1 force-displacement curve (compression test)

The peak force slightly higher than R40 1 is about 112,727 N (N = 112,000 per the data wedge), which speaks of industrial fiber performance that is evidently superior to recycled in a compression test.

The post-peak curve descends more slowly than the reference specimen, similar to R40 1, thus confirming higher ductility and energy dissipation. A longer plateau or an absence of sudden failure can also be seen in the curve, which may indicate improved fiber-matrix bond strength and load redistribution conferred by the industrial fibers. The I40_1 sample has exceeded both Ref 1 and R40 1, having the highest for parameter compressive strength and peak force among the three, thus indicating industrial fibers stand stronger reinforcement.

5.2. Comparison between industrial and recycled fibers

Results obtained from the three points bending test:

Table 13 results from the three point bending test

ID sample	F_{max} [N]	R_m [N/mm ²]
Ref 1	1657.57	4.00
Ref 2	1804.54	4.19
Ref 3	1963.83	4.52
R40 1	2780.98	6.46
R40 2	2057.98	4.89
R40 3	1862.41	4.31
I40 1	2749.77	6.38
I40 2	2745.98	6.51
I40 3	2569.89	5.92
R60 1	3805.25	8.63
R60 2	3060.83	6.85
R60 3	3716.74	8.35
I60 1	2810.06	6.28
I60 2	3415.15	7.50
I60 3	4594.50	10.41

In the context of a bending test, R_m typically refers to the flexural strength, also called the modulus of rupture (MOR). It is the maximum tensile stress experienced by the material. This value is calculated from the peak load during the bending test and provides an estimate of the material's ability to resist bending forces before failure.

For a three-point bending test, R_m is calculated using the following formula:

$$\frac{3 * P_{max} * L}{2 * b * h^2} \quad (5.1)$$

- R_m = Flexural strength or modulus of rupture (N/mm^2)
- P_{max} = Maximum applied load (N)
- L = Span length (distance between supports, mm)
- b = Width of the specimen (mm)
- h = Height (thickness) of the specimen (mm)

The group of samples with recycled fibers (R) has been observed to have more variability in max force values, where some of these show a significantly higher range from others (e.g., R60_1 at 3805.25 N and R60_2 at 3060.83 N).

The group with industrial fibers (I) shows a more steady behavior in the tests, with F_{max} values close in range (e.g., I60_1 at 2810.06 N, I60_2 at 3415.15 N, and I60_3 at 4594.50 N).

The recycled fibers, indeed, show good performance in some cases, especially at higher concentrations when the R60 samples are a real competitor in terms of flexural strength and maximum force. The results for samples R40 show lower strengths and higher variability, which might be associated with some irregularities in fiber distribution or properties.

Industrial Fibers (I):

The industrial fibers are the ones that kept showing better performance pretty regularly, especially in terms of flexural strength (I40 and I60).

The very high R_m values of I60 suggest an ability to disperse loading and enhance reinforcement better. The industrial fibers show somewhat lower maximum forces than the best recycled fiber samples, at least in some instances.

Compression test results:

Table 14 compression test results

ID sample	F_{max} [N]	R_m [N/mm ²]
Ref 1	99392.4	79.1
Ref 2	96766.9	77.0
Ref 3	91785.1	73.0
R40 1	110194.0	87.7
R40 2	110216.5	87.7
R40 3	108895.4	86.7
I40 1	112727.4	89.7
I40 2	106193.8	84.5
I40 3	112434.1	89.5
R60 1	104977.1	83.5
R60 2	104796.3	83.4
R60 3	105316.3	83.8
I60 1	113653.5	90.4
I60 2	108656.9	86.5
I60 3	112041.7	89.2

The machine applies a controlled compressive force to the fractured sample until it fails.

The compressive strength is calculated using the formula:

$$R_m = \frac{F_{max}}{S_0} \quad (5.2)$$

- F_{max} : maximum compressive force applied (N)

- S_0 : Initial cross-sectional area of the sample (mm²)

General Observations

Maximum Force (F_{max} [N]):

All tested industrial fiber (I) samples produced higher force values than the recycled fiber (R) samples.

For example, I60 sample series produce some of the highest force values of 113653.5 N for I60 1 and 112041.7 N for I60 3, while the R60 samples exhibit slightly lower values clustered from 104977.1-105316.3 N.

Industrial fiber (I) samples are found to have a greater compressive strength than recycled fibers (R). The highest R_m was found to be of 90.4 N/mm² from I60_1 and also the highest R_m values from I-class samples of I40_1 and I40_3 are greater than 89 N/mm².

Results for recycled fibers (R) are again lower, especially for series R60 (e.g., R60_1: 83.5 N/mm², R60_2: 83.4 N/mm²).

To have a better view of the results and their trend based on tested samples, these two histograms were plotted, both clearly show an increasing trend of the values throughout both compression and bending. The order of the bars follows the tables reported above, going from reference samples with no reinforcement, which means an RI of 0%, while the other samples have an RI of 40% and 60%, it can be clearly seen in both the plots that with a higher amount of fibers there is an improvement in strength.

The I60 samples consistently show the highest strength, both in bending and compression tests. Some variability in individual sample results suggests the presence of experimental uncertainties.

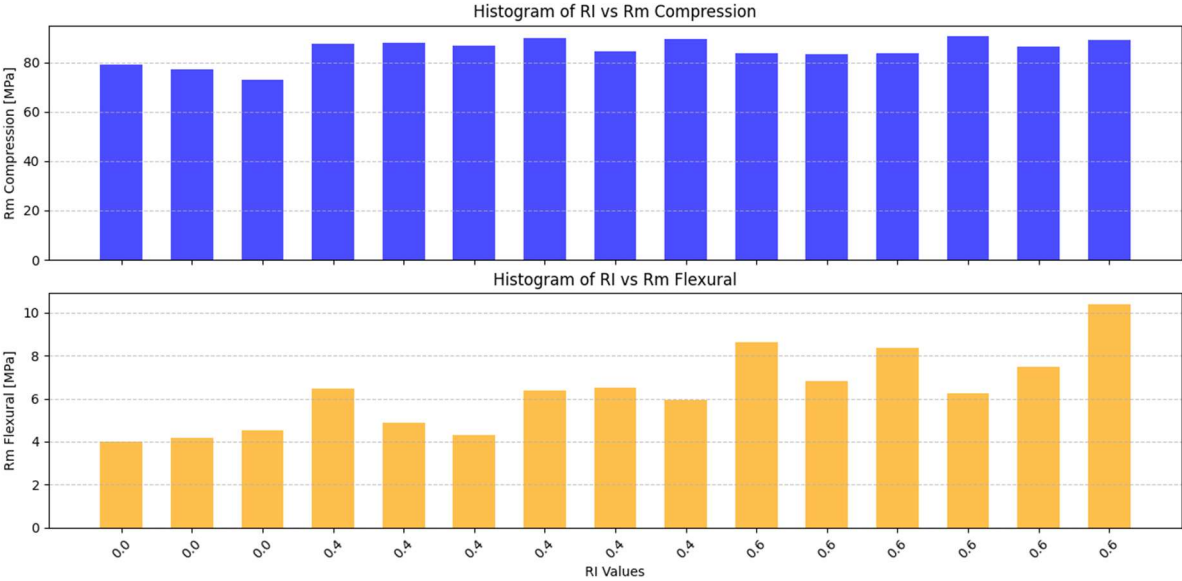


Figure 47 histograms RI vs Rm flexural and compression

The plot shown in picture 47 are obtained through a python code reported in APPENDIX A.

To make a comparison between the recycled and industrial fibers, the R40 series is stronger than the R60 series, with R40 1 and 40 2 both recording 87.7 N/mm², which is comparable to some results for industrial fibers.

Within the R60 series, the strength values are less than those for I60, with Rm values between 83.4 and 83.8 N/mm²."

The I40 series performed excellently, with Rm values close to or above 89 N/mm² for I40 1 and I40_3."

The I60 series consistently outperforms with the highest compression strength (I60 1: 90.4 N/mm²) and high Fmax values, thereby indicating a much better efficiency in reinforcing under compression.

Under bending tests, the R60 series showed competitive performance and up to 8.63 N/mm² Rm values, but these performed poorly in compression compared to industrial fibers, which had Rm values peaking at 83.8 N/mm².

Such variability in performance is related to the uneven distribution in terms of diameters and length of the fibers dispersed in the mortar.

In both bending and compression tests, industrial fibers consistently achieved higher and more reliable results. For example, the I60 series excelled in bending (up to 10.41 N/mm²) and compression (up to 90.4 N/mm²). Conversely to recycled fibers industrial ones have constant diameter and length which makes them more reliable in terms of results consistency.

In conclusion Industrial fibers (I) outperform recycled fibers (R) in both bending and compression tests, with the I60 series demonstrating the highest strengths overall. Their performance is more consistent making them preferable for high-performance applications.

On the other hand, recycled fibers still represent a very good option for reinforcement since there were improvements in terms of resistance, it is a greener product, much cheaper and sustainable in structural applications.

5.3. Tensile strenght

The tensile strenght tests were not done, but since the three point bending gave flexural strenght values , following the italian law and the european one, here reported the formulas:

1. Formula Eurocode 2:

$$f_{ctm,fl} \approx \max \left\{ \left(1.6 - \frac{h}{1000} \right) * f_{ctm}; f_{ctm} \right\} \quad [32] \quad (5.3)$$

Where:

$f_{ctm,fl}$ is the mean flexural tensile strenght

f_{ctm} is the mean direct tensile strenght

2. Formula (NTC 2018):

$$f_{ctm} \approx \frac{f_{cfm}}{1.2} \quad [33] \quad (5.4)$$

Where:

f_{ctm} is the mean direct tensile strenght

f_{cfm} is the mean flexural strenght

f_{cfm} has been estimated as the mean value for the 15 sample, with a result of 6.3 [N/mm²]

For the first formula it was applied the inverse calculation , here the results for both formulas:

$$f_{ctm,fl} = 4.1 \text{ [N/mm}^2\text{]}$$

$$f_{ctm} = 5.3 \text{ [N/mm}^2\text{]}$$

Chapter 6

Broken samples sections investigation

6.1. Fibers influence on broken sections

It was shown in previous chapters that as a consequence of the three points bending test the FRM samples went under failure and broke in two sections, one was used for compression tests while the other ones have been taken under further investigation, aiming to find a relationship between the broken sections characteristics and their structural performance.



Figure 48 broken samples

The aim is to evaluate how the fibers in the broken sections are distributed and how many are shown as well, furthermore trying to demonstrate if there is a correlation between such characteristic and the compression strength of the mortar.

In order to make this possible, a sintetic parameter needs to be established, but first:

$$th = \frac{A * V_f}{A_f} \quad [34] \quad (6.1)$$

-Where “th” is the theoretical number of fibers that appear in the fracture surface of a given specimen[34]

-A is the cross-section of the specimen [34]

$-A_f$ is the section of one fiber [34]

For what regards the section of the industrial fibers, the area was easily obtained since all the fibres have the same diameter, but for the recycled ones more steps were needed.

First of all, of every single fibers the diameter was available, because previously measured, for every fiber on Excel the area has been calculated and , at the end, the mean of the all areas was obateined. It was such mean that was used in the ‘th’ formula, with a value of 0.084mm^2 , smaller than the industrial fibers with an area of 0.125mm^2 .

Now, to estimate the theoretical number of fibers, it was necessary to calculate the area of the recycled fibers, as well as for the industrial ones.

The calculations to estimate ‘th’ for all the cases have been implemented on Matlab and can be seen in the Appendix A.

As a reminder, the V_f changes in all cases since there has been used two RI and two types of fibers with different aspect ratios are used.

R40_1

1	2	1
3	2	13
6	6	5

R40_2

1	0	1
3	1	3
3	5	6

R40_3

2	4	3
1	0	1
0	1	0

R60_1

3	3	5
3	3	6
2	3	5

R60_2

3	4	2
3	3	6
7	4	1

R60_3

4	5	0
3	4	0
6	3	0

I40_1

1	1	7
0	5	7
1	1	6

I40_2

1	0	8
0	3	6
1	2	5

I40_3

0	2	0
3	2	5
6	5	3

I60_1

5	0	0
7	4	0
4	4	1

I60_2

4	5	2
1	12	5
2	1	3

I60_3

4	5	3
2	7	5
1	1	2

Not all sections have fibers distributed uniformly, some quadrants are densely populated with fibers, and others are almost devoid of them.

This kind of uneven distribution would point to some stress concentrations or weak areas in the material, which, in fact, were failure initiation sites.

Some quadrants always have fiber concentrations above average, for wise, upper left in R40_1 and R60_3, upper right in 140_1 and 140_2, bottom left in 140_3.

These hotspots may indicate fiber regions that were maximizing resistance to other stress forces or where fibers were withdrawn during the event of failure. Moreover, some quadrants, especially the upper right and lower right, are often less populated with fibers or have none at all.

These sparse zones could indicate regions of weakness with the materials, which, in turn, would lead to the material's crack propagation or an outright failure.

In the studied sections, to have a better understanding of how fibers in the broken samples influence the structural performance, it was also measured, with an electronic caliper, the diameter of the fibers in millimeters, in every quadrant, in fact, bigger diameters should give a bigger bridging effect, potentially enhancing the bending resistance of the samples. Here reported the maximum and minimum values for every quadrant:

R40_1 (mm)

0.22	0.22	0.21
0.23		
0.39	0.14	0.28
		0.31
0.11	0.23	0.31
0.33		0.34

R40_2 (mm)

0.12		0.33
0.34	0.21	0.34
0.19	0.23	0.29
0.13	0.27	0.32

R40_3(mm)

0.16	0.22	0.25
0.29	0.38	0.59
0.35	0	0.30
0	0.29	0

R60_1 (mm)

0.23		
0.94		
0.20	0.35	
0.33	0.20	
0.21	0.18	0.33
	0.29	

R60_2 (mm)

0.25	0.39	0.45
0.39	0.36	0.34
0.33	0.43	0.56
0.40		

R60_3 (mm)

0.32	0.41	0
0.26	0.16	0
0.36	0.40	
0.33	0.23	0
0.50	0.26	

Regarding how the diameters are distributed along the broken sections, in some points was not possible to take measurements due to the fibers position within the matrix. Moreover, since only the samples with recycled fibers had different diameters dispersed in the matrix, it would have been useless to measure the diameters of the industrial fibers since they are all the same.

In the quadrants reported above, it was reported the maximum and minimum values of the fibers diameters for every quadrant of each sample, reminding that the mean diameter is about 0.29mm , some values exceeded and others went lower to the average.

There is an high chance that where the diameters were higher than the mean value, these were areas which played a bigger role in bridging the cracks and enhancing the resistance of the samples, leading to a better overall performance. Conversely, in the quadrants where the diameters are below the average value, might be areas which behaved as weak parts for resistance and bridging effect.

6.2. Relationship between beta, gamma and structural performance

The real number of fibers, counted in every cross section, will be reported as “n”, the ratio with the theoretical number will be called ‘β’:

$$\beta = \frac{n}{th} \quad [34] \quad (6.2)$$

The synthetic parameter ‘beta’ represents the ratio between the theoretical number of fibers and the counted one.

Table 15 beta estimation

ID	n	th	beta
R40_1	25	89	0.20
R40_2	23	89	0.19
R40_3	14	89	0.11
R60_1	33	133	0.18
R60_2	23	133	0.13
R60_3	26	133	0.14
140_1	29	102	0.28
140_2	29	102	0.28
140_3	26	102	0.25
160_1	39	153	0.25
160_2	35	153	0.23
160_3	30	153	0.20

From the tables above, it can be seen that the values of beta is far below one, since the number of counted fibers on the broken sections are very few compared to the theoretical ones, this discrepancy might be a consequence of the superplasticizer, as well as the fact that no fibers were pulled out during the test, keeping ‘n’ very low.

In order to estimate a potential relationship between the structural performance of the samples and the distribution of the fibers on the broken sections, it was decided to put on a graph the number of fibers and the resistance values obtained from the tests, but only for bending test, since there is very low correlation between compression and fibers effect, the plots are both shown below.

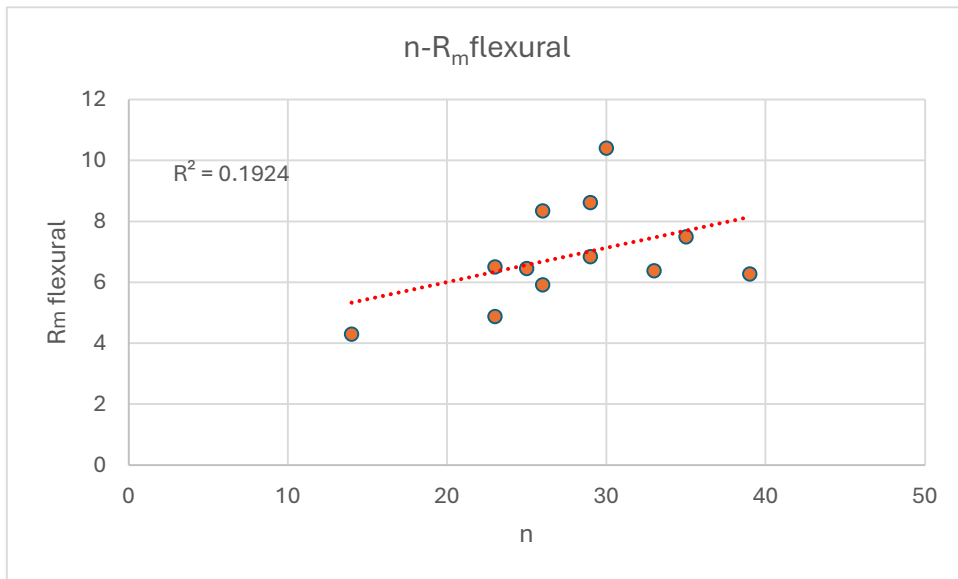


Figure 49 n-R_m flexural

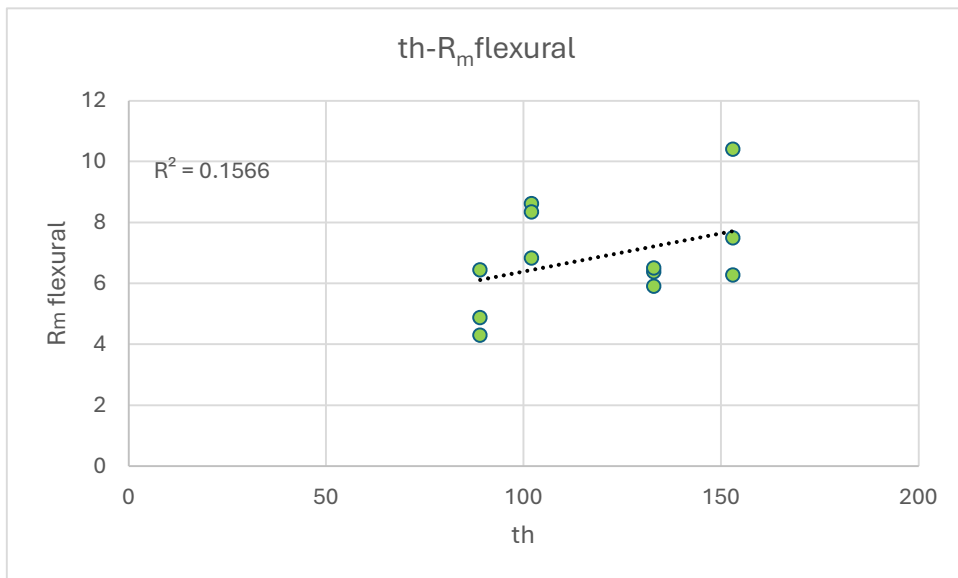


Figure 50 th- R_m flexural

Since the reliability for both the plots has been estimated, the ratio of the two can be used to evaluate the quality of the mix design that was done, and how far from an optimal behavior the process went.

Gamma is a parameter, defined as:

$$\varphi = \frac{R_{th}^2}{R_n^2} \quad (6.3)$$

- R_{th}^2 is the reliability for the theoretical number of fibers on the broken section
- R_n^2 is the reliability for the real number of fibers on the broken section

For the case study it came out a value of 0.156 for the theoretical values and 0.192 for the real number of fibers, the ratio, which is gamma, came out with a value of 0.81, that is a good result, since it is lower than 1, vice versa if it was bigger than one, the result would have been poor.

The plot indicates that there is almost a linear relationship between the parameter and flexural strength (R_m). So, with the increase in the number of fibers, R_m values also increase, suggesting that the structural behavior of the system under a bending moment increases with the increase of both 'th' and 'n'

Even though a relationship is shown, the values are not uniformly distributed around the trend line but slightly scattered.

The difference in compression resistance could be explained by another operating factor such as internal microstructural characteristics of the fiber-reinforced matrix, bond strength, or local stress distribution.

The contrasting relationships indicate that Beta is not a reliable predictor of both flexural behavior and compressive strength. This aligns with the mechanics of FRM materials, where bending stresses are highly dependent on section geometry and surface integrity, while compression relies more on internal structure and global material properties.

For design applications, focusing on gamma might be more beneficial for predicting and optimizing bending performance, but additional parameters may be required to accurately model compression behavior.

Chapter 7

Conclusions

The investigation sought to evaluate the Recycled Steel Fibers (RSF) and Industrial Steel Fibers used in constructing Fiber-Reinforced Mortars (FRM) in regard to mechanical performance, sustainability, and potential construction applications.

The work demonstrates the far better enhancement of the mechanical properties of mortars by putting in steel fibers, especially the ones that were recycled from end-of-life tires but also the benefit of environmental sustainability, all of which were worth the endeavor. The addition of steel fibers on both recycled and industrial types increased the flexural strength and compressive strength of mortars. The fiber-reinforced samples demonstrated post-crack ductility through fiber bridging of crack and retaining some strength, thereby prolonging the time until ultimate failure.

Industrial fibers consistently produced better mechanical performance than the recycled fiber, with higher peak loads and more consistent results. However, there was still a significant improvement compared to unreinforced mortars; it would be viable for use in some applications with recycled fibers.

Recycled steel fibers (RSF) provide a sustainable solution for reprocessing waste resources from end-of-life tires while incurring minimal environmental impact and complying with circular economy principles. RSF is cost-effective too and so becomes a very attractive option for large construction when sustainability and cost are key factors.

From the study, it was evident that fiber distribution in the mortar matrix was non-uniform, meaning that regions with large fiber concentrations had more importance in terms of resistance, while there were other regions with very scarce concentration of fibers.

Such uneven distribution led to differences in the mechanical performance, notably in bending since it was such a property where fibers played a crucial role.

Based on their astonishing properties, performance fiber-reinforced mortars can possibly be used for various construction activities such as structural repair, thin overlay application, and seismic retrofitting. The ductile nature and crack-resistant formation of mortars classify it as the best solution to users in harsh environments with high loading.

The combination of alkali-activated fly ash/slag (AAFS) mortars with steel fibers appears promising for applications like self-sensing, including stress monitoring and crack detection.

Further investigation will concentrate on optimizing the mix design and fiber distribution that can result in maximized advantages for any recycled fiber. Assessment of the long-term durability and performance of RSF under aggressive environments, i.e. reaction with the chemicals or subject to freeze-thaw cycles, is another area that can prove beneficial.

Development of hybrid fiber systems using a combination of recycled and industrial fibers could serve a balance between performance, sustainability, and cost.

As final thoughts, this work has proved that the fibers from AGR, are worth to be used in construction field, the analysis got positive results and demonstrated great enhancing in structural applications, mixtures with such type of product could serve as a beneficial green product , moving towards more sustainable options. This suggests that achieving a level of compromise between mechanical performance and sustainability versus cost is highly desirable when it comes to designing advanced construction materials. This research makes yet another small contribution to the ever-increasing library of sustainable construction practices.

APPENDIX A

1-MATLAB CODE USED IN CHAPTER THREE

```
% Lunghezza
mean_L = mean(L); % Media
std_L = std(L); % Deviazione standard
median_L = median(L); % Mediana
range_L = range(L); % Range
% Diametro
mean_D = mean(D);
std_D = std(D);
median_D = median(D);
range_D = range(D);
%%
% Plotting histograms and probability density
figure;
% Subplot for Length
subplot(1, 2, 1); % 1 row, 2 columns, 1st plot
histogram(L, 'Normalization', 'pdf', 'FaceColor', 'b'); % Histogram normalized to PDF
xlabel('Length (mm)');
ylabel('Probability Density');
title('Distribution of Lengths');
% Subplot for Diameter
subplot(1, 2, 2); % 1 row, 2 columns, 2nd plot
histogram(D, 'Normalization', 'pdf', 'FaceColor', 'r'); % Histogram normalized to PDF
xlabel('Diameter (mm)');
ylabel('Probability Density');
title('Distribution of Diameters');
% Adjust layout
sgtitle('Probability Density of Length and Diameter'); % Shared title for both subplots
%%
% Mostra i parametri
disp('Parametri statistici per la lunghezza:');
disp(table(mean_L, std_L, median_L, range_L));
disp('Parametri statistici per il diametro:');
disp(table(mean_D, std_D, median_D, range_D));
%grafico di dispersione
```

```

figure(2);
scatter(L, D, 'filled');
title('scatter plot lenght vs diameter');
xlabel('Lenght (mm)');
ylabel('Diameter (mm)');
grid on;
%Calcolo della correlazione
correlation = corr(L, D);
disp(['Coefficiente di correlazione tra lunghezza e diametro: ', num2str(correlation)]);
%%
%rapporto d'aspetto
R = L ./ D;
mean_R = mean(R);    % Media
std_R = std(R);      % Deviazione standard
cv_R = std_R / mean_R; % Coefficiente di variazione
med_R = median(R);   % Mediana
iqr_R = iqr(R);      % Interquartile range
disp(['Media: ', num2str(mean_R)]);
disp(['Deviazione standard: ', num2str(std_R)]);
disp(['Coefficiente di variazione: ', num2str(cv_R)]);
disp(['Mediana: ', num2str(med_R)]);
disp(['Range interquartile: ', num2str(iqr_R)]);
%% --- Aspect Ratio Analysis ---
% Calcolo del rapporto d'aspetto
R = L ./ D;

% Crea la figura
figure;
% Range per i fit del rapporto d'aspetto
x_vals_R = linspace(min(R), max(R), 100);
% Subplot 1: Istogramma del rapporto d'aspetto
subplot(2, 2, 1);
histogram(R, 'Normalization', 'pdf', 'EdgeColor', 'none');
title('Histogram of Aspect Ratio (L/D)');
xlabel('Aspect Ratio (L/D)');
ylabel('Probability Density');
grid on;
% Subplot 2: Normal Distribution Fit (Aspect Ratio)

```

```

subplot(2, 2, 2);
histogram(R, 'Normalization', 'pdf', 'EdgeColor', 'none');
hold on;
dist_R_norm = fitdist(R, 'Normal'); % Normal Fit
pdf_vals_R_norm = pdf(dist_R_norm, x_vals_R);
plot(x_vals_R, pdf_vals_R_norm, 'r', 'LineWidth', 2);
title('Normal Distribution Fit');
xlabel('Aspect Ratio (L/D)');
ylabel('Probability Density');
legend('Histogram', 'Normal', 'Location', 'best');
grid on;
hold off;
% Subplot 3: Lognormal Distribution Fit (Aspect Ratio)
subplot(2, 2, 3);
histogram(R, 'Normalization', 'pdf', 'EdgeColor', 'none');
hold on;
dist_R_log = fitdist(R, 'Lognormal'); % Lognormal Fit
pdf_vals_R_log = pdf(dist_R_log, x_vals_R);
plot(x_vals_R, pdf_vals_R_log, 'g', 'LineWidth', 2);
title('Lognormal Distribution Fit');
xlabel('Aspect Ratio (L/D)');
ylabel('Probability Density');
legend('Histogram', 'Lognormal', 'Location', 'best');
grid on;
hold off;
% Subplot 4: Weibull Distribution Fit (Aspect Ratio)
subplot(2, 2, 4);
histogram(R, 'Normalization', 'pdf', 'EdgeColor', 'none');
hold on;
dist_R_weibull = fitdist(R, 'Weibull'); % Weibull Fit
pdf_vals_R_weibull = pdf(dist_R_weibull, x_vals_R);
plot(x_vals_R, pdf_vals_R_weibull, 'm', 'LineWidth', 2);
title('Weibull Distribution Fit');
xlabel('Aspect Ratio (L/D)');
ylabel('Probability Density');
legend('Histogram', 'Weibull', 'Location', 'best');
grid on;
hold off;

```

```

% Aggiungi un titolo globale per la figura
sgtitle('Statistical Analysis of Aspect Ratio (L/D)');
%% --- Analysis for Diameter ---
figure;
% Range for PDF fitting for Diameter
x_vals_D = linspace(min(D), max(D), 100);
% Subplot 1: Histogram of Diameter
subplot(2, 2, 1);
histogram(D, 'Normalization', 'pdf', 'EdgeColor', 'none');
title('Histogram of Diameter');
xlabel('Diameter (mm)');
ylabel('Probability Density');
grid on;
% Subplot 2: Normal Distribution Fit (Diameter)
subplot(2, 2, 2);
histogram(D, 'Normalization', 'pdf', 'EdgeColor', 'none');
hold on;
dist_D_norm = fitdist(D, 'Normal'); % Normal Fit
pdf_vals_D_norm = pdf(dist_D_norm, x_vals_D);
plot(x_vals_D, pdf_vals_D_norm, 'r', 'LineWidth', 2);
title('Normal Distribution Fit');
xlabel('Diameter (mm)');
ylabel('Probability Density');
legend('Histogram', 'Normal', 'Location', 'best');
grid on;
hold off;
% Subplot 3: Lognormal Distribution Fit (Diameter)
subplot(2, 2, 3);
histogram(D, 'Normalization', 'pdf', 'EdgeColor', 'none');
hold on;
dist_D_log = fitdist(D, 'Lognormal'); % Lognormal Fit
pdf_vals_D_log = pdf(dist_D_log, x_vals_D);
plot(x_vals_D, pdf_vals_D_log, 'g', 'LineWidth', 2);
title('Lognormal Distribution Fit');
xlabel('Diameter (mm)');
ylabel('Probability Density');
legend('Histogram', 'Lognormal', 'Location', 'best');
grid on;

```

```

hold off;
% Subplot 4: Weibull Distribution Fit (Diameter)
subplot(2, 2, 4);
histogram(D, 'Normalization', 'pdf', 'EdgeColor', 'none');
hold on;
dist_D_weibull = fitdist(D, 'Weibull'); % Weibull Fit
pdf_vals_D_weibull = pdf(dist_D_weibull, x_vals_D);
plot(x_vals_D, pdf_vals_D_weibull, 'm', 'LineWidth', 2);
title('Weibull Distribution Fit');
xlabel('Diameter (mm)');
ylabel('Probability Density');
legend('Histogram', 'Weibull', 'Location', 'best');
grid on;
hold off;
% Add a global title for the figure
sgtitle('Statistical Analysis of Diameter');
%% --- Analysis for Length ---
figure;
% Range for PDF fitting for Length
x_vals_L = linspace(min(L), max(L), 100);
% Subplot 1: Histogram of Length
subplot(2, 2, 1);
histogram(L, 'Normalization', 'pdf', 'EdgeColor', 'none');
title('Histogram of Length');
xlabel('Length (mm)');
ylabel('Probability Density');
grid on;
% Subplot 2: Normal Distribution Fit (Length)
subplot(2, 2, 2);
histogram(L, 'Normalization', 'pdf', 'EdgeColor', 'none');
hold on;
dist_L_norm = fitdist(L, 'Normal'); % Normal Fit
pdf_vals_L_norm = pdf(dist_L_norm, x_vals_L);
plot(x_vals_L, pdf_vals_L_norm, 'r', 'LineWidth', 2);
title('Normal Distribution Fit');
xlabel('Length (mm)');
ylabel('Probability Density');
legend('Histogram', 'Normal', 'Location', 'best');

```

```

grid on;
hold off;
% Subplot 3: Lognormal Distribution Fit (Length)
subplot(2, 2, 3);
histogram(L, 'Normalization', 'pdf', 'EdgeColor', 'none');
hold on;
dist_L_log = fitdist(L, 'Lognormal'); % Lognormal Fit
pdf_vals_L_log = pdf(dist_L_log, x_vals_L);
plot(x_vals_L, pdf_vals_L_log, 'g', 'LineWidth', 2);
title('Lognormal Distribution Fit');
xlabel('Length (mm)');
ylabel('Probability Density');
legend('Histogram', 'Lognormal', 'Location', 'best');
grid on;
hold off;
% Subplot 4: Weibull Distribution Fit (Length)
subplot(2, 2, 4);
histogram(L, 'Normalization', 'pdf', 'EdgeColor', 'none');
hold on;
dist_L_weibull = fitdist(L, 'Weibull'); % Weibull Fit
pdf_vals_L_weibull = pdf(dist_L_weibull, x_vals_L);
plot(x_vals_L, pdf_vals_L_weibull, 'm', 'LineWidth', 2);
title('Weibull Distribution Fit');
xlabel('Length (mm)');
ylabel('Probability Density');
legend('Histogram', 'Weibull', 'Location', 'best');
grid on;
hold off;
% Add a global title for the figure
sgtitle('Statistical Analysis of Length');
figure;
% Range for PDF fitting for Diameter
x_vals_D = linspace(min(D), max(D), 100);
% Subplot 1: Histogram of Diameter
subplot(2, 2, 1);
histogram(D, 'Normalization', 'pdf', 'EdgeColor', 'none');
title('Histogram of Diameter');
xlabel('Diameter (mm)');

```

```

ylabel('Probability Density');
grid on;
% Subplot 2: Normal Distribution Fit (Diameter)
subplot(2, 2, 2);
histogram(D, 'Normalization', 'pdf', 'EdgeColor', 'none');
hold on;
dist_D_norm = fitdist(D, 'Normal'); % Normal Fit
pdf_vals_D_norm = pdf(dist_D_norm, x_vals_D);
plot(x_vals_D, pdf_vals_D_norm, 'r', 'LineWidth', 2);
title('Normal Distribution Fit');
xlabel('Diameter (mm)');
ylabel('Probability Density');
legend('Histogram', 'Normal', 'Location', 'best');
grid on;
hold off;
% Subplot 3: Lognormal Distribution Fit (Diameter)
subplot(2, 2, 3);
histogram(D, 'Normalization', 'pdf', 'EdgeColor', 'none');
hold on;
dist_D_log = fitdist(D, 'Lognormal'); % Lognormal Fit
pdf_vals_D_log = pdf(dist_D_log, x_vals_D);
plot(x_vals_D, pdf_vals_D_log, 'g', 'LineWidth', 2);
title('Lognormal Distribution Fit');
xlabel('Diameter (mm)');
ylabel('Probability Density');
legend('Histogram', 'Lognormal', 'Location', 'best');
grid on;
hold off;
% Subplot 4: Weibull Distribution Fit (Diameter)
subplot(2, 2, 4);
histogram(D, 'Normalization', 'pdf', 'EdgeColor', 'none');
hold on;
dist_D_weibull = fitdist(D, 'Weibull'); % Weibull Fit
pdf_vals_D_weibull = pdf(dist_D_weibull, x_vals_D);
plot(x_vals_D, pdf_vals_D_weibull, 'm', 'LineWidth', 2);
title('Weibull Distribution Fit');
xlabel('Diameter (mm)');
ylabel('Probability Density');

```

```

legend('Histogram', 'Weibull', 'Location', 'best');
grid on;
hold off;
% Add a global title for the figure
sgtitle('Statistical Analysis of Diameter');
%% Quantitative test
% Perform Anderson-Darling test for Normal, Lognormal, and Weibull distributions
% Normal distribution test
[h_L_norm, p_L_norm] = adtest(L, 'Distribution', 'normal');
[h_D_norm, p_D_norm] = adtest(D, 'Distribution', 'normal');
% Lognormal distribution test
[h_L_lognorm, p_L_lognorm] = adtest(L, 'Distribution', 'lognormal');
[h_D_lognorm, p_D_lognorm] = adtest(D, 'Distribution', 'lognormal');
% Weibull distribution test (Weibull is not directly supported in adtest)
% We approximate by fitting Weibull parameters and transforming the data
param_L = wblfit(L);
param_D = wblfit(D);
[h_L_weibull, p_L_weibull] = adtest(L ./ param_L(1), 'Distribution', 'extreme value');
[h_D_weibull, p_D_weibull] = adtest(D ./ param_D(1), 'Distribution', 'extreme value');
% Print results
fprintf('\n==== Anderson-Darling Test Results ==== \n');
fprintf('\nFor L vector: \n');
fprintf(' Normal Fit: h = %d, p = %.4f \n', h_L_norm, p_L_norm);
fprintf(' Lognormal Fit: h = %d, p = %.4f \n', h_L_lognorm, p_L_lognorm);
fprintf(' Weibull Fit: h = %d, p = %.4f \n', h_L_weibull, p_L_weibull);
fprintf('\nFor D vector: \n');
fprintf(' Normal Fit: h = %d, p = %.4f \n', h_D_norm, p_D_norm);
fprintf(' Lognormal Fit: h = %d, p = %.4f \n', h_D_lognorm, p_D_lognorm);
fprintf(' Weibull Fit: h = %d, p = %.4f \n', h_D_weibull, p_D_weibull);
%% Pearson test
% Perform Pearson Chi-Square Goodness-of-Fit Test (chi2gof)
% Normal distribution test
[h_L_norm_chi, p_L_norm_chi] = chi2gof(L, 'CDF', makedist('Normal', 'mu', mean(L), 'sigma',
std(L)));
[h_D_norm_chi, p_D_norm_chi] = chi2gof(D, 'CDF', makedist('Normal', 'mu', mean(D), 'sigma',
std(D)));
% Lognormal distribution test
[h_L_lognorm_chi, p_L_lognorm_chi] = chi2gof(L, 'CDF', makedist('Lognormal', 'mu',
mean(log(L)), 'sigma', std(log(L))));

```

```

[h_D_lognorm_chi, p_D_lognorm_chi] = chi2gof(D, 'CDF', makedist('Lognormal', 'mu',
mean(log(D)), 'sigma', std(log(D))));
% Weibull distribution test
param_L_wbl = wblfit(L);
param_D_wbl = wblfit(D);
[h_L_weibull_chi, p_L_weibull_chi] = chi2gof(L, 'CDF', makedist('Weibull', 'a', param_L_wbl(1), 'b',
param_L_wbl(2)));
[h_D_weibull_chi, p_D_weibull_chi] = chi2gof(D, 'CDF', makedist('Weibull', 'a', param_D_wbl(1),
'b', param_D_wbl(2)));
% Print results
fprintf('\n==== Pearson Chi-Square Test Results ==== \n');
fprintf('\nFor L vector: \n');
fprintf(' Normal Fit: h = %d, p = %.4f \n', h_L_norm_chi, p_L_norm_chi);
fprintf(' Lognormal Fit: h = %d, p = %.4f \n', h_L_lognorm_chi, p_L_lognorm_chi);
fprintf(' Weibull Fit: h = %d, p = %.4f \n', h_L_weibull_chi, p_L_weibull_chi);
fprintf('\nFor D vector: \n');
fprintf(' Normal Fit: h = %d, p = %.4f \n', h_D_norm_chi, p_D_norm_chi);
fprintf(' Lognormal Fit: h = %d, p = %.4f \n', h_D_lognorm_chi, p_D_lognorm_chi);
fprintf(' Weibull Fit: h = %d, p = %.4f \n', h_D_weibull_chi, p_D_weibull_chi);
%%
% Compute Aspect Ratio
AR = L ./ D;
% AndDarling Test for AR
[h_AR_norm_ad, p_AR_norm_ad] = adtest(AR, 'Distribution', 'normal');
[h_AR_lognorm_ad, p_AR_lognorm_ad] = adtest(AR, 'Distribution', 'lognormal');
[h_AR_weibull_ad, p_AR_weibull_ad] = adtest(AR, 'Distribution', 'weibull');
% Pearson Chi-Square Test for AR
[h_AR_norm_chi, p_AR_norm_chi] = chi2gof(AR, 'CDF', makedist('Normal', 'mu', mean(AR),
'sigma', std(AR)));
[h_AR_lognorm_chi, p_AR_lognorm_chi] = chi2gof(AR, 'CDF', makedist('Lognormal', 'mu',
mean(log(AR)), 'sigma', std(log(AR))));
param_AR_wbl = wblfit(AR);
[h_AR_weibull_chi, p_AR_weibull_chi] = chi2gof(AR, 'CDF', makedist('Weibull', 'a',
param_AR_wbl(1), 'b', param_AR_wbl(2)));
% Print Results
fprintf('\n==== Anderson-Darling Test Results for AR ==== \n');
fprintf(' Normal Fit: h = %d, p = %.4f \n', h_AR_norm_ad, p_AR_norm_ad);
fprintf(' Lognormal Fit: h = %d, p = %.4f \n', h_AR_lognorm_ad, p_AR_lognorm_ad);
fprintf(' Weibull Fit: h = %d, p = %.4f \n', h_AR_weibull_ad, p_AR_weibull_ad);

```

```

fprintf('\n==== Pearson Chi-Square Test Results for AR ==== \n');
fprintf(' Normal Fit: h = %d, p = %.4f\n', h_AR_norm_chi, p_AR_norm_chi);
fprintf(' Lognormal Fit: h = %d, p = %.4f\n', h_AR_lognorm_chi, p_AR_lognorm_chi);
fprintf(' Weibull Fit: h = %d, p = %.4f\n', h_AR_weibull_chi, p_AR_weibull_chi);
%%
param_L_wbl = wblfit(L);
param_D_wbl = wblfit(D);
[h_L_norm_chi, p_L_norm_chi] = chi2gof(L, 'CDF', makedist('Normal', 'mu', mean(L), 'sigma',
std(L)));
[h_L_lognorm_chi, p_L_lognorm_chi] = chi2gof(L, 'CDF', makedist('Lognormal', 'mu',
mean(log(L)), 'sigma', std(log(L))));
[h_L_weibull_chi, p_L_weibull_chi] = chi2gof(L, 'CDF', makedist('Weibull', 'a', param_L_wbl(1), 'b',
param_L_wbl(2)));
[h_D_norm_chi, p_D_norm_chi] = chi2gof(D, 'CDF', makedist('Normal', 'mu', mean(D), 'sigma',
std(D)));
[h_D_lognorm_chi, p_D_lognorm_chi] = chi2gof(D, 'CDF', makedist('Lognormal', 'mu',
mean(log(D)), 'sigma', std(log(D))));
[h_D_weibull_chi, p_D_weibull_chi] = chi2gof(D, 'CDF', makedist('Weibull', 'a', param_D_wbl(1),
'b', param_D_wbl(2)));
fprintf('\n==== Pearson Chi-Square Test Results ==== \n');
fprintf('L: Normal Fit: h = %d, p = %.4f | Lognormal Fit: h = %d, p = %.4f | Weibull Fit: h = %d, p =
%.4f\n', h_L_norm_chi, p_L_norm_chi, h_L_lognorm_chi, p_L_lognorm_chi, h_L_weibull_chi,
p_L_weibull_chi);
fprintf('D: Normal Fit: h = %d, p = %.4f | Lognormal Fit: h = %d, p = %.4f | Weibull Fit: h = %d, p =
%.4f\n', h_D_norm_chi, p_D_norm_chi, h_D_lognorm_chi, p_D_lognorm_chi, h_D_weibull_chi,
p_D_weibull_chi);

```

-2 PYTHON CODE USED FOR CHAPTER FIVE

```

import numpy as np
import matplotlib.pyplot as plt
# Define the given vectors
RI = np.array([0, 0, 0, 0.4, 0.4, 0.4, 0.4, 0.4, 0.4,
              0.6, 0.6, 0.6, 0.6, 0.6, 0.6])

Rm_Compression = np.array([79.09, 77.00, 73.04, 87.69, 87.70, 86.65, 89.70, 84.50, 89.47,
                          83.53, 83.39, 83.80, 90.44, 86.46, 89.15])

Rm_Flexural = np.array([4.00, 4.18, 4.52, 6.45, 4.88, 4.30, 6.38, 6.51, 5.92,
                       8.62, 6.84, 8.35, 6.27, 7.50, 10.40])

```

```

# Convert RI to categorical labels
RI_labels = [str(r) for r in RI]
# Define bar width
bar_width = 0.
# Create figure with 2 subplots
fig, ax = plt.subplots(2, 1, figsize=(12, 8), sharex=True)
# Plot for Rm Compression
ax[0].bar(range(len(RI)), Rm_Compression, width=bar_width, color='blue', alpha=0.7)
ax[0].set_ylabel('Rm Compression [MPa]')
ax[0].set_title('Histogram of RI vs Rm Compression')
ax[0].grid(axis='y', linestyle='--', alpha=0.7)
# Plot for Rm Flexural
ax[1].bar(range(len(RI)), Rm_Flexural, width=bar_width, color='orange', alpha=0.7)
ax[1].set_xlabel('RI Values')
ax[1].set_ylabel('Rm Flexural [MPa]')
ax[1].set_title('Histogram of RI vs Rm Flexural')
ax[1].grid(axis='y', linestyle='--', alpha=0.7)
# Set x-axis labels to match RI values
ax[1].set_xticks(range(len(RI)))
ax[1].set_xticklabels(RI_labels, rotation=45)
# Adjust layout and show plot
plt.tight_layout()
plt.show()

```

-3 MATLAB CODE USED IN CHAPTER 6

```

thR40=(0.0047*1600) / (0.084);
thR60=(0.0070*1600)/(0.084);
thI40=(0.0080*1600)/(0.40^2*pi /4);
thI60=(0.0120*1600)/(0.40^2*pi /4);

```

REFERENCES

- [1] J. Manso-Morato, N. Hurtado-Alonso, V. Revilla-Cuesta, M. Skaf, and V. Ortega-López, “Fiber-Reinforced concrete and its life cycle assessment: A systematic review,” Oct. 01, 2024, *Elsevier Ltd.* doi: 10.1016/j.jobbe.2024.110062.
- [2] R. D. Woodson, “Materials and methods for repair and rehabilitation,” *Concrete Structures*, pp. 61–81, Jan. 2009, doi: 10.1016/B978-1-85617-549-4.00006-X.
- [3] C. Selin Ravikumar, V. Ramasamy, and T. S. Thandavamoorthy, “Effect of Fibers In Concrete Composites,” 2015. [Online]. Available: <http://www.ripublication.com>
- [4] L. A. Le, G. D. Nguyen, H. H. Bui, A. H. Sheikh, and A. Kotousov, “Incorporation of micro-cracking and fibre bridging mechanisms in constitutive modelling of fibre reinforced concrete,” *J Mech Phys Solids*, vol. 133, p. 103732, Dec. 2019, doi: 10.1016/j.jmps.2019.103732.
- [5] “4. PROTOCOLLO DI CALCOLO NTC 2018.”
- [6] E. Denneman, E. P. Kearsley, and A. T. Visser, “Splitting tensile test for fibre reinforced concrete,” *Materials and Structures/Materiaux et Constructions*, vol. 44, no. 8, pp. 1441–1449, Oct. 2011, doi: 10.1617/s11527-011-9709-x.
- [7] P. Kaur and M. Talwar, “Different types of Fibres used in FRC,” 2017. [Online]. Available: www.ijarcs.info
- [8] V. Ráček, J. Vodička, and V. Vytlačilová, “Examples of Use of FRC with Recycled Concrete in Structures,” in *Procedia Engineering*, Elsevier Ltd, 2016, pp. 337–344. doi: 10.1016/j.proeng.2016.07.381.
- [9] M. Lu, H. Xie, H. Wang, and Y. Ma, “Self-sensing properties of steel fiber reinforced-alkali-activated fly ash/slag mortar,” *Constr Build Mater*, vol. 458, Jan. 2025, doi: 10.1016/j.conbuildmat.2024.139580.
- [10] H. Xu *et al.*, “Experimental study on durability of fiber reinforced concrete: Effect of cellulose fiber, polyvinyl alcohol fiber and polyolefin fiber,” *Constr Build Mater*, vol. 306, p. 124867, Nov. 2021, doi: 10.1016/j.conbuildmat.2021.124867.
- [11] H. Xu *et al.*, “Experimental study on durability of fiber reinforced concrete: Effect of cellulose fiber, polyvinyl alcohol fiber and polyolefin fiber,” *Constr Build Mater*, vol. 306, p. 124867, Nov. 2021, doi: 10.1016/J.CONBUILDMAT.2021.124867.
- [12] “Consiglio Superiore dei Lavori Pubblici Servizio Tecnico Centrale Linea guida per l’identificazione, la qualificazione, la certificazione di valutazione tecnica ed il controllo di accettazione dei calcestruzzi fibrorinforzati FRC (Fiber Reinforced Concrete).”
- [13] D. R. S and B. P. Annapurna, “FIBER REINFORCED MORTAR”, [Online]. Available: <http://ymerdigital.com>
- [14] Sabireen *et al.*, “Mechanical performance of fiber-reinforced concrete and functionally graded concrete with natural and recycled aggregates,” *Ain Shams Engineering Journal*, vol. 14, no. 9, Sep. 2023, doi: 10.1016/j.asej.2023.102121.
- [15] M. Esmailzade, M. Eskandarinia, and F. Aslani, “Effect of impurities of steel fibers extracted from shredded tires on the behavior of fiber-reinforced concrete,” *Structures*, vol. 45, pp. 1175–1188, Nov. 2022, doi: 10.1016/j.istruc.2022.09.088.

- [16] A. Zia, P. Zhang, and I. Holly, "Experimental investigation of raw steel fibers derived from waste tires for sustainable concrete," *Constr Build Mater*, vol. 368, p. 130410, Mar. 2023, doi: 10.1016/j.conbuildmat.2023.130410.
- [17] M. A. Aiello, F. Leuzzi, G. Centonze, and A. Maffezzoli, "Use of steel fibres recovered from waste tyres as reinforcement in concrete: Pull-out behaviour, compressive and flexural strength," *Waste Management*, vol. 29, no. 6, pp. 1960–1970, Jun. 2009, doi: 10.1016/j.wasman.2008.12.002.
- [18] G. Romeo, "Data analysis for business and economics," *Elements of Numerical Mathematical Economics with Excel*, pp. 695–761, Jan. 2020, doi: 10.1016/B978-0-12-817648-1.00013-X.
- [19] A. Alrawashdeh and O. Eren, "Mechanical and physical characterisation of steel fibre reinforced self-compacting concrete: Different aspect ratios and volume fractions of fibres," *Results in Engineering*, vol. 13, p. 100335, Mar. 2022, doi: 10.1016/j.rineng.2022.100335.
- [20] Y. Qi, B. Jiang, W. Lei, Y. Zhang, and W. Yu, "Reliability Analysis of Normal, Lognormal, and Weibull Distributions on Mechanical Behavior of Wood Scrimber," *Forests*, vol. 15, no. 9, p. 1674, Sep. 2024, doi: 10.3390/f15091674.
- [21] A. Maydeu-Olivares and C. García-Forero, "Goodness-of-Fit Testing," in *International Encyclopedia of Education, Third Edition*, Elsevier, 2009, pp. 190–196. doi: 10.1016/B978-0-08-044894-7.01333-6.
- [22] M. Saculinggan and E. A. Balase, "Empirical Power Comparison Of Goodness of Fit Tests for Normality In The Presence of Outliers," *J Phys Conf Ser*, vol. 435, p. 012041, Apr. 2013, doi: 10.1088/1742-6596/435/1/012041.
- [23] A. F. Siegel, "Hypothesis Testing," in *Practical Business Statistics*, Elsevier, 2016, pp. 255–295. doi: 10.1016/B978-0-12-804250-2.00010-9.
- [24] Q. Yuan, Z. Liu, K. Zheng, and C. Ma, "Portland cement concrete," in *Civil Engineering Materials*, Elsevier, 2021, pp. 59–204. doi: 10.1016/B978-0-12-822865-4.00003-9.
- [25] Y.-C. Ou, M.-S. Tsai, K.-Y. Liu, and K.-C. Chang, "Compressive Behavior of Steel-Fiber-Reinforced Concrete with a High Reinforcing Index," *Journal of Materials in Civil Engineering*, vol. 24, no. 2, pp. 207–215, Feb. 2012, doi: 10.1061/(asce)mt.1943-5533.0000372.
- [26] C. M. Ho, S. I. Doh, X. Li, S. C. Chin, and T. Ashraf, "RSM-based modelling of cement mortar with various water to cement ratio and steel slag content," *Physics and Chemistry of the Earth, Parts A/B/C*, vol. 128, p. 103256, Dec. 2022, doi: 10.1016/j.pce.2022.103256.
- [27] UNI ente italiano di Normazione, *EN 196-1:2016 Methods of testing cement*. 2016.
- [28] Z. Zhu *et al.*, "An Experimental Study of the Mechanical Properties of Partially Rehabilitated Cable Tunnels," *Materials*, vol. 15, no. 14, Jul. 2022, doi: 10.3390/ma15144830.
- [29] M. Sood and G. Dwivedi, "Effect of fiber treatment on flexural properties of natural fiber reinforced composites: A review," *Egyptian Journal of Petroleum*, vol. 27, no. 4, pp. 775–783, Dec. 2018, doi: 10.1016/j.ejpe.2017.11.005.
- [30] C. Wang and C. C. Sun, "A critical examination of three-point bending for determining Young's modulus," *Int J Pharm*, vol. 629, p. 122409, Dec. 2022, doi: 10.1016/j.ijpharm.2022.122409.

- [31] Mardoqueu M. Costa, “Compression Testing: Exploring Methods, Applications, and Benefits”.
- [32] “Eurocodice 2-Progettazione delle strutture di calcestruzzo Parte 1-1: Regole generali e regole per gli edifici ENV 1992-1-1.”
- [33] P. R. T E P R I M A and P. G. Verdi, “GAZZETTA UFFICIALE DELLA REPUBBLICA ITALIANA DIREZIONE E REDAZIONE PRESSO IL MINISTERO DELLA GIUSTIZIA-UFFICIO PUBBLICAZIONE LEGGI E DECRETI-VIA ARENULA, 70-00186 ROMA AMMINISTRAZIONE PRESSO L’ISTITUTO POLIGRAFICO E ZECCA DELLO STATO-VIA SALARIA, 691-00138 ROMA-CENTRALINO 06-85081-LIBRERIA DELLO STATO Aggiornamento delle «Norme tecniche per le costruzioni»,” 2018.
- [34] A. Enfedaque, M. G. Alberti, and J. C. Gálvez, “Influence of fiber distribution and orientation in the fracture behavior of polyolefin fiber-reinforced concrete,” *Materials*, vol. 12, no. 2, Jan. 2019, doi: 10.3390/ma12020220.